Compact MZI Switch Modulator for Visible Wavelengths

A Thesis submitted by

Suresh Chand Jat

2015PWC5398

Under the guidance of
Dr. M. Ravi Kumar

In partial fulfillment for the award of the degree of

MASTER OF TECHNOLOGY

to the

DEPARTMENT OF ELECTRONICS AND COMMUNICATION ENGINEERING

MALAVIYA NATIONAL INSTITUTE OF TECHNOLOGY

JAIPUR, RAJASTHAN 302017

(JUNE 2017)

Certificate

This is to certify that thesis entitled "**Compact MZI Switch Modulator for Visible Wavelengths**" which is submitted by **SURESH CHAND JAT (2015PWC5398)** in partial fulfilment of requirement for degree of **Master of Technology in Wireless & Optical Communication Engineering** submitted to **MALAVIYA NATIONAL INSTITUTE OF TECHNOLOGY JAIPUR** is a record of student's own work carried out under my supervision. The matter in this report has not been submitted to any university or institution for the award of any degree.

Dr. M. Ravi Kumar

(Project Supervisor)

Assistant Professor

Dept. of Electronics and Communication Engineering

MNIT Jaipur 302017

Date:

Place:

Declaration

I **Suresh Chand Jat** hereby declare that this thesis submission titled as '**Compact MZI Switch Modulator for Visible Wavelengths,'** is my own work and that, to the best of my knowledge and belief.

It contains no material previously published or written by another person, nor material which to be substantial extent has been accepted for the award of any other degree by university or other institute of higher learning.

Wherever I used data (Theories, results) from other sources, credit has been made to that sources by citing them (to the best of my knowledge). Due care has been taken in writing this thesis, errors and omissions are regretted.

Date: **Suresh Chand Jat**

Place: ID: 2015PWC5398

Acknowledgment

I would like to thank all peoples who have helped me in this project, directly or indirectly.

I am especially grateful to my supervisor ***Dr. M. Ravi Kumar*** *(Assistant Professor, Dept. of ECE, MNIT Jaipur) for his invaluable guidance during my project work, encouragement to explore parallel paths and freedom to pursue my ideas. My association with him has been a great learning experience. He made it possible for me to discuss with a number of people and work in different areas.*

I express my sincere gratitude to Professor K.K. Sharma (Head of Department) for his support and guidance in this research work. Many thanks to committee members Dr. Ghanshyam Singh (Associate Professor), Dr. Vijay Janyani (Associate Professor), Dr. Ritu Sharma (Associate Professor) and Mr Ashish Kumar Ghunawat (Assistant Professor) for their valuable comments and guidance in research exploration, without this guidance it was not possible to achieve these good results in this research work. I would like to thank Mr. Vijay Singh and Mr. Dipak for allowing me in laboratories over time.

I am also very thankful to my friends Sanjay Kumar Sharma, Anil Kumar Jangir, Fateh Lal Lohar, Harsh Kumar, Dinesh Kumawat, Dipika Baria, Ishwar Kumawat, Pankaj Kathania and Laxman Kumar for their valuable suggestions and discussion, which I had with them about this research work. They also help me in designing work of my project.

I would also like to thank Ministry of HRD, Government of India for its support to me to pursue my Masters in Wireless and Optical Communication Engineering from Malaviya National Institute of Technology, Jaipur. This support provided me library, laboratory, hostel and other related infrastructure.

- *Suresh Chand Jat*

List of Abbreviations

2D	-	*2 Dimensions*
3D	-	*3 Dimensions*
ADI	-	*Alternate Direction Implicit*
ADP	-	*Ammonium Dihydrogen Phosphate*
BER	-	*Bit Error Rate*
BPM	-	*Beam Propagation Method*
BPSK	-	*Binary Phase Shift Keying*
CAD	-	*Computer Added Design*
CFM	-	*Correlation Function Methods*
DC	-	*Direct Current*
ER/ Ex.R	-	*Extinction Ratio*
FTTB	-	*Fiber to the Building*
FTTC	-	*Fiber to the Curb*
FTTH	-	*Fiber to the Home*
IL	-	*Insertion Loss*
IR	-	*Infrared*
KDP	-	*Potassium Dihydrogen Phosphate*
LAN	-	*Local Area Network*
LED	-	*Light Emitting Diode*
LiNbO3	-	*Lithium Niobate*
MW	-	*Mega Watt*
MZ	-	*Mach-Zehnder*
MZI	-	*Mach-Zehnder Interferometer*
NRZ-OOK	-	*Non-Return to Zero On-Off Keying*
O-E-O	-	*Optical-Electrical-Optical Conversion*
PLM	-	*Perfectly Matched Layer*
RI	-	*Refractive Index*
RZ-OOK	-	*Return to Zero On-Off Keying*

SNR	-	*Signal to Noise Ratio*
TBC	-	*Transparent Boundary Condition*
TE	-	*Transverse Electrical*
Ti: LiNbO3	-	*Titanium diffused Lithium Niobate*
TM	-	*Transverse Magnetic*
TMM	-	*Transfer Matrix's Methods*
VLC	-	*Visible light Communication*
Wi-Fi	-	*Wireless Fidelity*

List of symbols

$^{\circ}C$	-	*Degree centigrade*
μm	-	*Micrometre*
d	-	*Distance between Electrodes*
dB	-	*Decibel*
D_H	-	*Lateral diffusion length*
D_V	-	*Diffusion length depth*
K	-	*Kerr Coefficient*
L	-	*Length of Electrode Region*
mm	-	*Millimetre*
mW	-	*Milli watt*
n	-	*Refractive Index*
n_e	-	*Extraordinary refractive index*
nm	-	*Nanometre*
n_o	-	*Ordinary refractive index*
n_x	-	*Refractive index in x direction*
n_y	-	*Refractive index in y direction*
P_{in}	-	*Power at input*
P_{off}	-	*Power at output for output low or '0'*
P_{on}	-	*Power at output for output high or '1'*
P_{out}	-	*Power at output*
r_{ij}	-	*Electro-Optic Tensor*
V	-	*Voltage*
Vcm	-	*Voltage. Centimetre*
V_π	-	*Switching Voltage*
$V_\pi L$	-	*Switching Voltage-Length Product*
Γ	-	*Phase difference retardation*
Δn	-	*Effective Refractive Index*
$\Delta\varphi$	-	*Phase change*
λ	-	*Wavelength*
P_{out1}	-	*Power at Out 1 port*
P_{out2}	-	*Power at Out 2 port*

List of Figures

List of Tables

Abstract

Electro-optic effect is widely used phenomenon in integrated optics to design and develop various kind of optical devices to be used for different applications in optical communication system. Lithium Niobate ($LiNbO_3$) is a material with a high electro-optic coefficient that means it shows a high amount of electro-optic effect. Titanium diffused Lithium Niobate (Ti: $LiNbO_3$) has more optical swiftness and bandwidth to design integrated optical devices. Ti: $LiNbO_3$ based Mach-Zehnder Interferometer modulators are used in optical communication for modulation at 1300 nm and 1550 nm wavelength.

Visible Light Communication (VLC) is the new trend in digital communication. In VLC, signal is transmitted in light form that means, in the range of 350 nm to 750 nm wavelength. Modulation in VLC is done in electrical domain by direct modulating electrical signal to transmitting LED, this modulation can be done in optical domain using MZI modulator structure.

In this thesis, we consider the design of compact Mach-Zehnder Interferometer (MZI) switch modulators for visible wavelengths to be used in Visible Light Communication for the modulation of light. Five new optimized designs have been developed. These designs are 33 mm long operates at 680 nm, 8 mm long operates at 680 nm, 6 mm long works on 610 nm, 4.5 mm long works on 515 nm and 4 mm long operates at 515 nm. In these modulator designs, two optimized designs with length 6 mm and 4 mm are more recommended for commercial use, operating at 610 nm and 515 nm wavelength respectively. For these two modulators, insertion loss is calculated and found to be 0.08 dB for 6 mm design and 0.47 dB for 4 mm design. The extinction ratio is 45.14 dB for 6 mm design and 25.34 dB for 4 mm design. The switching voltage-length product ($V\pi L$) is 1.35 Vcm for 6 mm design and 0.96 Vcm for the 4 mm design, which is low as compared to 6.75 Vcm for reported 33 mm design operating at 1300 nm wavelength.

Keywords— Visible Light Communication (VLC), Electro-Optic Effect, Titanium diffused Lithium Niobate (Ti: LiNbO3), Mach-Zehnder Interferometer (MZI) switch modulator, OptiBPM.

Contents

Chapter 1 **Introduction**

1.1 **Introduction and Motivation**

As the world is progressing fast the demand for high data rate is also increasing rapidly. In today's world every person desire for the higher data rate for his use, like video streaming, downloading, online gaming, augmented reality and for many other high ends uses. To compete with these demands all the backbone network is working on the optical fiber. Optical fiber provides the data rate in terms of Tera bit per seconds with very low transmission losses and better BER (Bit Error Rate) [1]. As the data rate demand increasing fiber network is reaching towards the customer end to fulfil these demands. Fiber to the building (FTTB), Fiber to the curb (FTTC) and Fiber to the home (FTTH) are the new use of fiber network to reach at the user end. We use local area network (LAN) and Wireless Fidelity (Wi-Fi) to provide indoor connection. For mobile devices, we use radio frequency wireless communication but it has data rate limitation of 100 Mbps and the signal can go outside the building walls. The need for Visible Light Communication (VLC) has emerged over the radio frequency wireless communication since it provides data security and the higher amount of data rate for a small area [2]. VLC for short range communication provides optical wireless communication as well as illuminance to the area by using visible wavelengths from 380 nm to 750 nm [3]. At present light emitting diodes (LED) are used to deliver the with illuminance in the VLC[4]. The modulation techniques for VLC are Return to Zero On-Off Keying (RZ-OOK), Non-Return to Zero On-Off Keying (NRZ-OOK) and Binary Phase Shift Keying (BPSK) in the electrical domain on the applied electrical signal at LED[5].

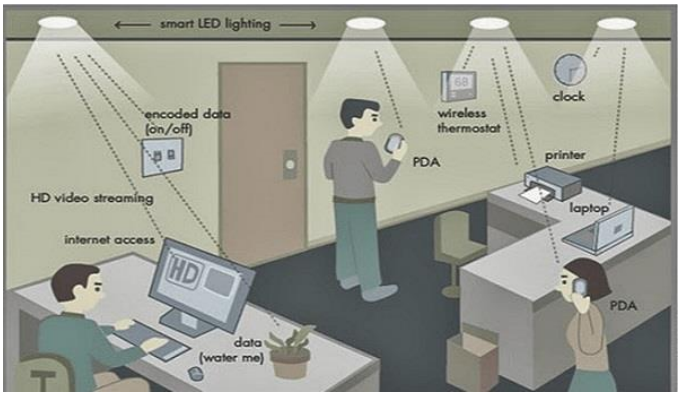

Figure 1-1: VLC demonstration for indoor communication

The use of Mach-Zehnder Interferometer (MZI) switch modulator for modulation in VLC may increase the data rate significantly. Titanium diffused Lithium Niobate (Ti: $LiNbO_3$) has been used as the material to design this modulator; Titanium diffused Lithium Niobate has the advantage of high electro-optic effect, acousto-optic effect and transmission characteristic in addition to the commercial availability of Lithium Niobate[6]. The MZI switch works on the electro-optic modulation process. Electro-optical modulation is based on the Pockels effect, in which an applied electrical field gives the variation in the phase of a propagating optical signal. This variation in the phase of propagating signal is directly proportional to the applied electrical field. This phase variation can be converted into the amplitude variation in the MZI structure or it can be used for switching purpose in same MZI structure. The current designs of MZI switch operate at 1550 nm and 1330 nm optical window and have the large push-pull MZI arm length and also high switching voltage-length product ($V_\pi L$). Hence the device length of 33 mm[7], [8] is large to make compact devices for VLC. Here we proposed the MZI switch modulator for visible wavelengths to be used in VLC for modulation purpose.

Various designs are created, from them, 6 mm and 4 mm designs are very compact and have very less value of switching voltage length multiplication ($V_\pi L$). These two designs also shown the high value of extinction ratio (Ex.R) and lower values of the insertion loss (IL). Previously available designs have the switching voltage-length multiplication as high as 6.75 Vcm [7] as compared to newly proposed devices with $V_\pi L$, 1.35 Vcm and 0.96 Vcm for 6 mm and 4 mm devices respectively. Available MZI switch modulator works on the 1300 nm and 1550 nm wavelengths for long haul communication[9], and these are fabricated on the Lithium Niobate. The proposed

devices operate in the visible wavelength spectrum of from 380 nm to 750 nm that means the modulated signal can directly be sent to the user device or the end terminal. Higher values of extinction ratio mean lower the chances of Bit Error Rate (BER) thus improved data rate for end users. A commercially used MZI modulator is shown in the Figure 1-2 below.

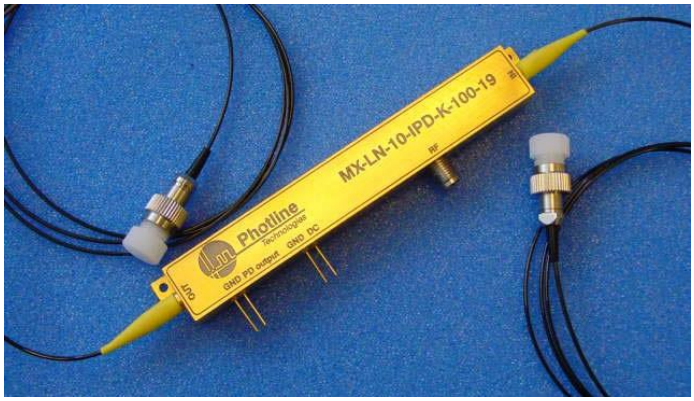

Figure 1-2: Commercially available MZI modulator

1.2 Objective

The purpose of this thesis work is to design the modulator for the visible light communication, so there the need of optical- electrical- Optical (O-E-O) can be eliminated. By eliminating the O-E-O conversion higher energy efficiency and higher data rate transmission may be achieved. The designed Modulator is to be capable of modulating the light signal with high extinction ratio and should have the minimum insertion loss. To develop the device, three parameters are kept at under observation and these are operating wavelength, extinction ratio and insertion loss. Limits for these three parameters are kept under following conditions (1) Operating wavelength from 380 nm to 750 nm, (2) Extinction ratio (Ex.R) more than 15 dB and (3) Insertion Loss (IL) Under the 1 dB.

While working on the above devices efforts are made to control the switching voltage (V_π) which is kept under the 8 V. Another important parameter switching voltage-length product is considered to design the device. Here we achieved very good results in term of voltage-length product which is lower than 2 Vcm for the designed devices. MZI Modulator designs are the new idea for modulation in the visible wavelengths because commercially available devices works on 1300 nm and have the switching voltage of 8V-

10 V range. Along with the above conditions following objectives are also considered in this project-

- Low switching voltage (V_π).
- Smaller size of the interferometer arms to reduce the size as well as the lower switching voltage length product.
- To give a basic idea for the modulation in optical domain for the visible light communication so that O-E-O conversion can be omitted.
- One of the objectives is to design modulator at visible wavelengths with various length from that which have the maximum extinction ratio and lower insertion loss can be chosen as the optimized device for the use in VLC.
- To discuss various important parameters in detail for the MZI switch modulator and the comparative study of these models with the previously available devices.

1.3 Thesis Organisation

This thesis is organized in total 6 chapters including this introductory chapter. Following the introduction, chapter 2 gives the basic idea about the Electro-optic effect in the dielectric material with the explanation of Pockels effect and Kerr effect. It also discusses the Electro-Optic Modulation and its types that are used in the integrated photonics.

In Chapter 3, the material characteristics of Lithium Niobate ($LiNbO_3$) and of the Titanium diffused Lithium Niobate (Ti: $LiNbO_3$) are explained. The MZI switch is described in details with its designing parameters and material available to design the MZI switch, along with this MZI modulator and its variants are discussed in brief. This chapter focuses on the reported MZI switch designs and modulators. In Chapter 4 basics of design tool OptiBPM have been presented with its working principles and simulation environment that it uses. In addition to this, the process of MZI switch designing has been discussed in details.

Chapter 5 gives detail analysis of designed MZI switch modulator designs. Various designing parameters and simulation parameters are discussed and detail analysis of

results have been given. Comparison of outcome parameters insertion loss, extinction ratio, V_π and the switching voltage-length product with the parameters of the previously available devices have been presented here.

In Chapter 6 thesis work have been concluded with some future aspects and direction for further work.

Chapter 2 **Electro-Optic Effect and Electro-Optic Modulation**

2.1 Introduction

This chapter gives an explanation of Electro-Optic Effect, Pockels effect and the electro-optic modulations with various configuration is given. It explains how the distortion produced in a crystal lattice by the application of an electric field affects the transmission of light through the crystal. The electro-optic effect is of significant practical importance as it can be used to amplitude and phase modulate light beams, change their frequencies and modify the direction in which they travel.

2.2 Electro-Optic Effect

The electro-optic effect is referred as a phenomenon in which when an external electrical field is applied to a material or photonic crystal, changes its optical property especially its refractive index[10]. In other words, when a strong electric fields applied to a material causes higher-order variations in the polarizability. If a strong DC field is applied across a material, the inner charges will be moved from their symmetry places. If a light wave now passes through the material, these charges will have the fewer choice to respond to the fluctuations of the wave's electric field. Electro-optic effects refer to the changes in a material's polarizability (and therefore its refractive index) by the occurrence of an external electric field[11][12]. These changes will be naturally anisotropic, based on the direction of the external field.

If these effects can be defined, to first order, as being linearly proportional to the applied field, then the crystal shows the linear electro-optic effect. We shall see that this results, only if the crystal lattice lacks a centre of symmetry. So, some cubic crystals can show the linear electro-optic effect[12]. If the crystal possesses a centre of symmetry (or is even an isotropic material such as a gas or liquid), a change in optical properties can result that depends, to first order, on the square of the applied field. This is the quadratic electro-optic effect. Both the linear and quadratic electro-optic effects can be used efficiently in various optical devices.

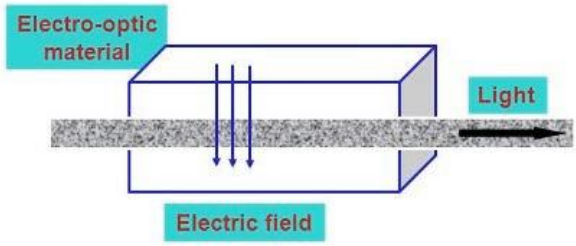

Figure 2-1: Electro-Optic Effect

The necessity of the refractive index on the applied electric field receipts one of following two forms:

- If refractive index changes in proportion to the applied electric field, then the effect is known as the linear electro-optic effect or the Pockels effect.
- If refractive index changes in proportion to the square of the applied electric field, then the effect is known as the quadratic electro-optic effect or the Kerr effect.

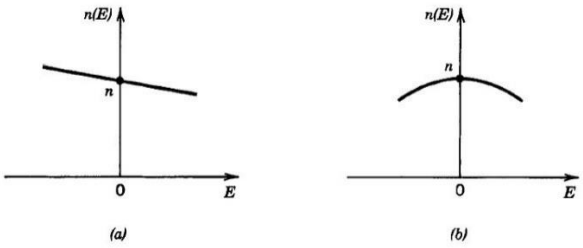

Figure 2-2: Variation of effective refractive index: (a) Pockels Effect, (b) Kerr Effect

The change in the refractive index is characteristically very small. But, its effect on an optical wave promulgating a distance much larger than a wavelength of light in the medium can be substantial. If the refractive index rises by 10^{-4}, for example, an optical wave pass on a distance of 10^4 wavelengths will experience an extra phase shift of 2π.

2.3 Principle of Electro-Optics

The refractive index of an electro-optic medium is a function *n(E)* of the applied electric field E. This function varies only slightly with E so that it can be expanded in a Taylor's series about E = 0

$$n(E) = n + a_1 E + \frac{1}{2} a_2 E^2 + \cdots \quad (1)$$

The change in n due to the first E term is called the Pockels effect $\Delta n = a_1 E$. And change in n due to the second E^2 term is known as the Kerr effect and $a_2 = \lambda K$ where K is called the Kerr coefficient, $\Delta n = a_2 E^2 = (\lambda K) E^2$.

In practice, only the first two terms of Taylor's series expansion are observed in materials. The first-order term is referred to as the linear electro-optic effect or Pockels Effect[13], and the second-order term is referred to as the quadratic electro-optic effect or Kerr effect[14].

Both of these two effects are explained in the following subsections.

2.4 Pockels Effect

In simple terms, the Pockels Effect describes the linear reliance of the refractive index on an applied field. More carefully, it describes changes to a crystal's major refractive indices because of applied field along a definite crystal direction, as it affects direction and polarization of given light[13]. The indicatrix of Lithium Niobate is shown below with and without applied electric field.

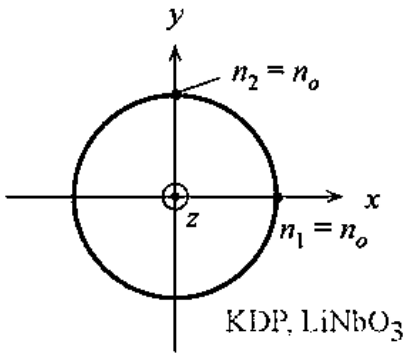

Figure 2-3: Optical indicatrix without electric field applied

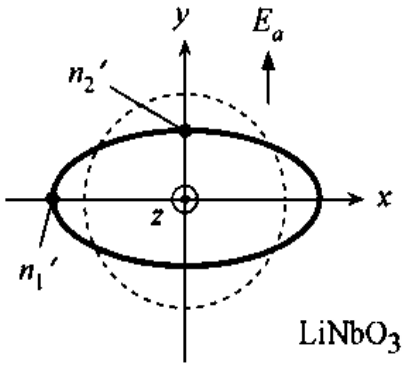

Figure 2-4: Optical field with applied electric field

The Pockels effect is a second order nonlinear optical occurrence and this only occurs in crystals which don't have inversion symmetry. For the linear electro-optic effect under an external electrical field E, the index ellipsoid is given as follow.

$$\left[\frac{1}{n_x^2}+\Delta\left(\frac{1}{n^2}\right)_1\right]x^2+\left[\frac{1}{n_y^2}+\Delta\left(\frac{1}{n^2}\right)_2\right]y^2+\left[\frac{1}{n_z^2}+\Delta\left(\frac{1}{n^2}\right)_3\right]z^2+2\Delta\left(\frac{1}{n^2}\right)_4 yz + 2\Delta\left(\frac{1}{n^2}\right)_5 xz+2\Delta\left(\frac{1}{n^2}\right)_6 xy=1 \quad (2)$$

The changes in the six coefficient of index ellipsoid are given below

$$\left(\Delta\left(\frac{1}{n^2}\right)_{1,2,3,4,5,6}\right)=\begin{pmatrix} r_{11} & r_{12} & r_{13} \\ r_{21} & r_{22} & r_{23} \\ r_{31} & r_{32} & r_{33} \\ r_{41} & r_{42} & r_{43} \\ r_{51} & r_{52} & r_{53} \\ r_{61} & r_{62} & r_{63} \end{pmatrix}\begin{pmatrix} E_x \\ E_y \\ E_z \end{pmatrix} \quad (3)$$

Here *r* is called as the electro-optic tensor and r_{ij} is the electro-optic coefficient or Pockels coefficient. The electro-optic tensor of Lithium Niobate is given by

$$r=\begin{pmatrix} 0 & -r_{22} & r_{13} \\ 0 & r_{22} & r_{13} \\ 0 & 0 & r_{33} \\ 0 & r_{51} & 0 \\ r_{51} & 0 & 0 \\ -r_{22} & 0 & 0 \end{pmatrix} \quad (4)$$

Lithium Niobate ($LiNbO_3$) is a material with a robust Pockels Effect, with 3m symmetry. Its non-zero tensor constants are r_{22} = 3.4 ($x10^{-12}$m/V) and r_{42} = 28 ($x10^{-}$

^{12}m/V). It is indeed uniaxial, and generally used as a substrate and waveguide in integrated optics

Linear Electro-optic effect is categorized in following two types-

- ✓ Longitudinal Electro-Optic Effect
- ✓ Transversal Electro-Optic Effect

In the longitudinal electro-optic effect, applied electric field is applied in the direction of the light propagating and in the transversal electro-optic effect applied field is perpendicular to the propagation direction of light.

Materials which shows the Pockels effect are KDP (KH_2PO_4, Potassium dihydrogen phosphate), ADP ($NH_4H_2PO_4$, Ammonium dihydrogen phosphate), $LiNbO_3$ (Lithium Niobate), $LiTaO_3$ (Lithium Tantalate), $BaTiO_3$ (Barium Titanate) and CdTe (Cadmium Telluride).

2.5 Kerr Effect

The Kerr Effect[14] is a second-order variation in the refractive index, this stint with the square of the applied field:

$$\Delta n = a_2 E^2 = (\lambda K) E^2$$

Unlike the Pockels Effect, all materials show the Kerr effect, including isotropic crystals, amorphous materials, and even liquids and covalently bonded solids. Instinctively, the Kerr effect is at ease to understand: a firm external field is applied in the same path as the light polarization. It distorts the equilibrium motion of inner charges, assertive them to the “limits of their travel" and making it “tougher" for them move in response to the light wave's external electric field. Theoretically, this decelerates down the wave and decreases the refractive index in this polarization plane. The light that is polarized vertically to the external field still has liberty to accelerate inner charges in the unhindered direction, and thus practices the original refractive index.

Practically talking, the Kerr effect is far weaker than the Pockels effect, so developing it requires very high field strengths. Kerr coefficient of some materials which shows the Kerr effect is shown below-

Table 2-1: Kerr Effect Coefficient of some materials (Source: Hecht, E., Optics, 4th Edition. Addison Wesley, San Francisco, 2002)

Material	**K (m/V^2 $x10^{-12}$)**
Benzene (C_6H_6)	0.006
Carbone Disulphide (CS_2)	0.035
Chloroform (CHC_{13})	-0.038
Water (H_2O)	0.052
Nitro toluene ($C_5H_7NO_2$)	1.37
Nitrobenzene ($C_6H_5NO_2$)	2.44

2.6 Electro-Optic Modulators

An electro-optic modulator is a basic working device to change the electrically induced refractive index or a change in natural birefringence[15]. Depending on the configuration of the device, the following properties of the fiber can be controlled varied: phase, polarization, amplitude, frequency or direction of propagation. The device is generally designed for optimal efficiency at a single wavelength, with some degradation of broadband performance or multimode lasers[11].

Electro-optical devices can be used in analog or digital format formats. The choice is dictated by the requirements of the system and the properties of the available components (fiber or sensor sources, etc.). Analog modulation requires high signal-to-noise (SNR), thus restraining its use in narrowband, short-range applications. Digital modulation, on the other hand, is higher bandwidth, long range carriers.

An electro-optical modulator may be classified into two types, longitudinal or transverse depending on how the voltage is applied with respect to the direction of propagation of light in the device. Basically, a bulk modulator comprises an electro-optical crystal sandwich between a pair of electrodes and can therefore be configured as a capacitor. In general, the input and output faces are parallel so that the beam subjected to a uniform phase moves section beams.

In the longitudinal configuration, a voltage is applied parallel to the direction of the wave vector as shown in Figure 2-5.

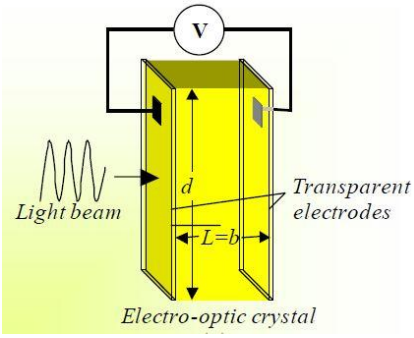

Figure 2-5: Longitudinal electro-optic modulator configuration

And the configuration of transversal electro-optic modulators is given in the following figure 2-6, where applied electrical field is perpendicular to the direction of the light propagation.

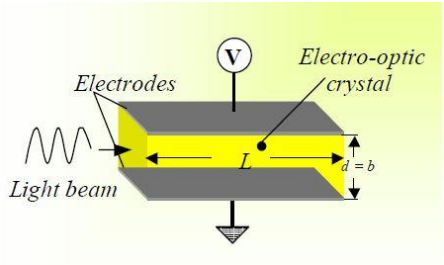

Figure 2-6: Transversal electro-optic modulator

The types of Electro-Optic Modulators is explained in the following subsections with brief details.

2.6.1 Phase Modulation

A light wave can be phase modulated without altering the polarization, or voltage by means of an electro-optical crystal and a polarizer to come into the correct configuration. An illustration of a longitudinal apparatus shown in Figure 2-7. In common, an applied voltage V will revolve the major axis of the cross-section of the crystal[16].

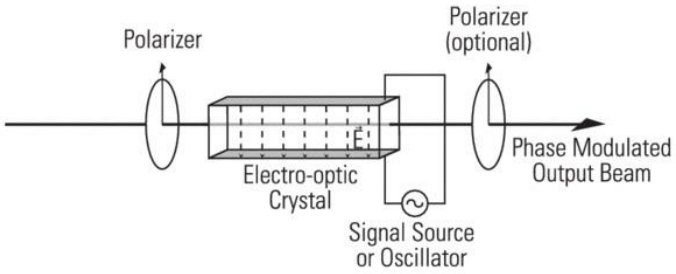

Figure 2-7: Longitudinal Phase Modulator

The voltage that would yield an induced phase shift of π is the half - wave voltage. It is $V_\pi=\lambda/n^3r$ for a longitudinal modulator and $V_\pi=\lambda/n^3r(d/L)$ for a transverse modulator.

2.6.2 Polarization Modulation (Dynamic Retardation)

Polarization modulations include the coherent addition of two orthogonal waves, which causes an alteration in state of input to output polarization. As for a phase modulator, the basic constituents for an electro-optical polarization modulator (or dynamic delay or polarization state converter) are an electro-optical crystal and an input polarizer.

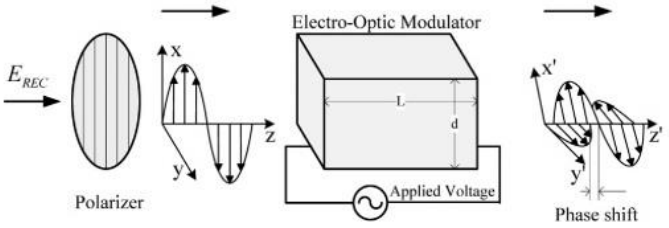

Figure 2-8: Polarization Modulation

Since the two polarizations are transmitted at dissimilar speeds through the crystal, a phase difference (Γ) or Γ retardation is developed as a function of the length.

$$\Gamma = \frac{2\pi}{\lambda}(n_{x'} - n_{y'})L \tag{5}$$

2.6.3 Amplitude Modulation

The intensity (optical power) of a light wave can be configured in different ways. Some options contain the use of (a) forming a dynamic delay with crossed polarizers at the output, (b) the dynamic deceleration configuration with polarizer parallel to the

output, (c)the configuration of the phase modulator in the interferometer Mach-Zehnder fraction, or (d) a dynamic retarder having push-pull electrodes.

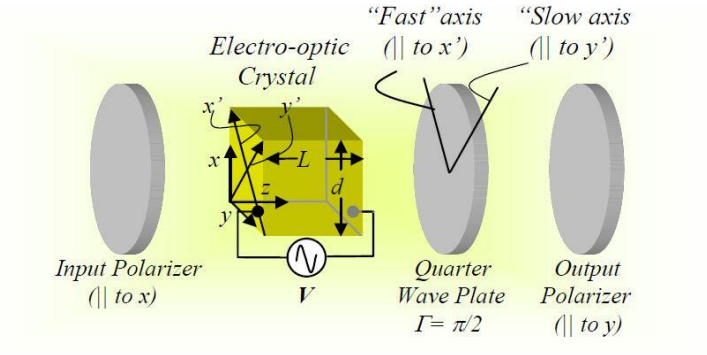

Figure 2-9: Longitudinal Amplitude Modulator

In amplitude modulation, the applied electric field of the modulation voltage is directly converted to the intensity modulation of light that can be further illustrated in the following diagram.

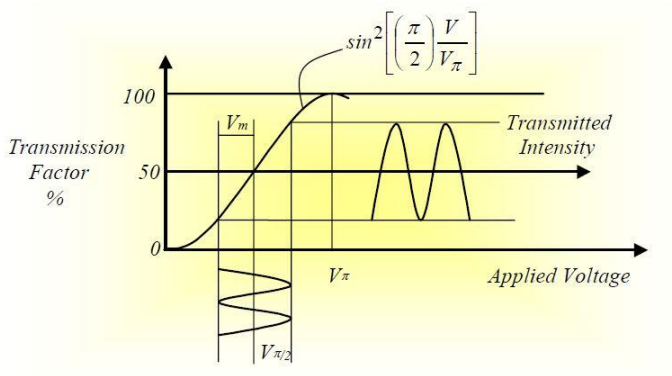

Figure 2-10: Direct amplitude modulation

2.6.4 Frequency Modulation

In the frequency modulation, shift or deviation is desirable in the frequency w_d of the instantaneous frequency w of the optical medium. A method for taking a frequency change is to use an amplitude modulator configuration of an electro-optical crystal among the left and right circular polarizers. The modulator electrodes must be designed to produce a circular electric field that is applied.

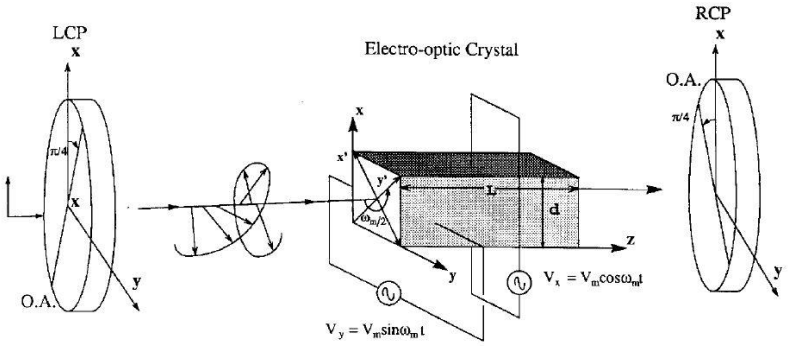

Figure 2-11: A frequency modulator using the phase modulator and two polarizers

In the above configuration, a shift in the frequency is obtained by rotating optical and applied electrical field in the opposite direction.

Chapter 3 Titanium Diffused Lithium Niobate (Ti: $LiNbO_3$) and MZI Switch Modulator

3.1 Introduction

In this chapter we are going to discuss about the electro-optic material Titanium diffused Lithium Niobate (Ti: $LiNbO_3$), the Lithium Niobate ($LiNbO_3$) is a material which shows high value of electro –optic coefficient and shows high ferroelectric effect. Along to this, we will study the basic Mach-Zehnder Interferometer (MZI) design. The variant of the MZI structure and MZI 2x2 switch is discussed in brief.

3.2 Lithium Niobate ($LiNbO_3$)

Lithium Niobate ($LiNbO_3$) was first discovered in 1949 as a ferroelectric material[17], it shows high amount of electro-optic effect means it's a good electro-optic material showing Pockels effect[15]. Pockels effect means linear electro-optic effect. Transparency of Lithium Niobate in near infrared range is very high and high value of electro-optic coefficient make it the perfect choice for wafer material in integrated photonics. It has high Curie temperature (1100-1180 ˚C) that makes it applied for creation of low-loss optical waveguides through diffusion of metals[18]. $LiNbO_3$ shows the stability in chemical, and mechanical properties also it's compatible with integrated circuit technology.

It is widely used ferroelectric material in these days because it has large electro-optic, photo-elastic, acousto-optic piezoelectric and pyroelectric coefficients. The nature of Lithium Niobate is birefringent. Lithium is a solid in its crystalline form, which is very steady at room temperature chemically fairly sensitive to a damp environment. In addition, it has enough hardness to handle regularly. The crystalline arrangement of this material at room temperature is the triangular 3 m. This makes the optically uniaxial crystal with two refractive indices n_e and n_o. Both pointers have values greater than 2 in the entire area of transparency, it is necessary in many cases, anti-reflective coatings on the optical surfaces to make.

The crystal structure of Lithium Niobate is shown in below figure with the axes information.

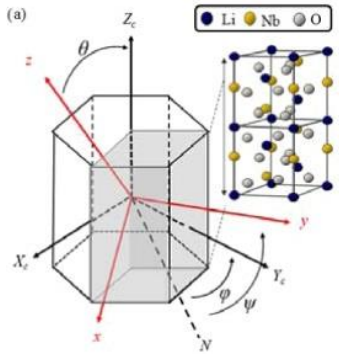

Figure 3-1: Lithium Niobate crystal structure

Some fundamental properties of Lithium Niobate[19] are listed in the following table.

Table 3-1: Physical and optical properties of Lithium Niobate

General properties	
Crystal Symmetry	Trigonal
Hardness	~ 5 Mohs
Melting point	1260 ˚C
Method of growth	Czochralski, large crystals
Stoichiometry	Nonstoichiometric, ~6% Li deficiency easy to dope in high concentration, Curie temperature TC = 1150 °C spontaneous polarization Ps(RT) ~96 C/m2 180° domains
Ferroelectricity	
Piezoelectric	
Pyroelectric	
Optical Properties	
Transparency region	Near IR (350 nm- ~5000 nm)
Optical anisotropy	Uniaxial, c axis
Refractive indices	n_o = 2.286, n_e = 2.203. (at 632.8 nm)
Optical homogeneity	~5 x 10^{-5}
Optical effects	Acousto-optic, electro-optic, second, order nonlinearity, bulk photovoltaic, effect, optical damage – photorefractive, effect
Optical damage threshold	250 MW/ cm^2

The linear electro-Optic effect is given by the relation

$$\Delta\left(\frac{1}{n^2}\right)_{ij} = \sum_k r_{ijk}\ E_k \tag{6}$$

Electro-optic tensor of $LiNbO_3$ is given by

$$r_{ijk} = \begin{pmatrix} 0 & -r_{22} & r_{13} \\ 0 & r_{22} & r_{13} \\ 0 & 0 & r_{33} \\ 0 & r_{51} & 0 \\ r_{51} & 0 & 0 \\ -r_{22} & 0 & 0 \end{pmatrix} \tag{7}$$

Here in the above expressions, *n* is refractive index effective and *r* is the electro-optic coefficient. Values of r_{13} = 10 pm/V, r_{33} = 32.2 pm/V, r_{22} = 6.7 pm/V and r_{51} = 32.6 pm/V for static electric field and light of 633 nm.

Optical waveguides which are produced on the Lithium Niobate are Titanium diffused $LiNbO_3$, Photon exchange $LiNbO_3$, TiPE $LiNbO_3$, Zn-diffused $LiNbO_3$, He^+ ion-implanted Lithium Niobate, H^+ ion implanted Lithium Niobate, and Si and other heavy ion implanted Lithium Niobate. For our MZI structure design, we used the Titanium diffused Lithium Niobate (Ti: $LiNbO_3$)[20].

3.3 Titanium Diffused Lithium Niobate (Ti: $LiNbO_3$)

For optical device fabrication Titanium diffused Lithium Niobate is the widely used optical waveguide material, most of the modulator devices and electro-optic circuits are designed by this material. The operating swiftness or bandwidth of the optical modulation device has recently been improved and the external modulators are prepared of Titanium diffused $LiNbO_3$ (Ti: $LiNbO_3$)[21]. The Titanium is diffused on the Lithium Niobate using the photolithography process. In the photolithography process, desired waveguide can be formed by some steps of fabrication. Titanium is diffused by E-beam, Evaporation or sputtering[22].

A significant benefit of this technology, in addition, to taking advantage of excellent electro-optical features, and acousto-optical conduction and the commercial obtainability of Lithium Niobate is that the diffusion procedure allows good control of the size mode

waveguide. This provides the flexibility to realize outstanding coupling ends to the single-mode optical fibers, where the corresponding of the fiber's mode size and the waveguide is critical. In fact, waveguide coupling losses of fewer than 0.3 dB were detected. From the similar scattering parameters, the propagation losses of the waveguide are 0.3 dB / cm for wavelengths in the range from 1.3 to 1.5μm. Lower fiber coupling losses are, of course, critical for applications in optical communication systems[23].

The use of Titanium diffused Lithium Niobate results in the lower value of switching voltage or half wave voltage (V_π) for the electro-optic modulator devices. Lower value of switching voltage means higher the power efficiency of the device.

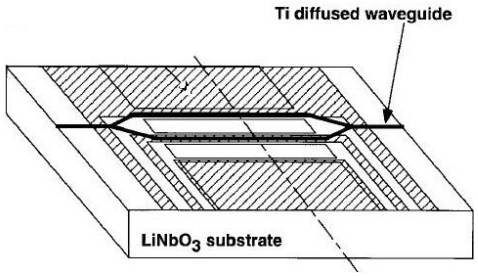

Figure 3-2: Ti diffused Lithium Niobate based MZ structure

3.4 Mach-Zehnder Interferometer (MZI)

Ludwig Mach and Ludwig Zehnder have developed the interferometer principle, so the name of this principle has been kept after their name as Mach-Zehnder Interferometer (MZI). In this structure phase shift gets developed in an arm of interferometer structure and then this phase shift is used to produce intensity or phase or frequency modulation in the traveling wave[12].

In optical fiber communicating system the Mach-Zehnder Interferometer principle is used in the integrated photonic devices. In integrated photonics, MZI modulators uses the Pockels effect for MZ principle realization[24]. Mainly there are three structures in the MZI design (1) Y-branch splitter and Y branch Combiner, (2) Y splitter branch and directional coupler combiner[25], and (3) Directional coupler splitter and directional coupler combiner.

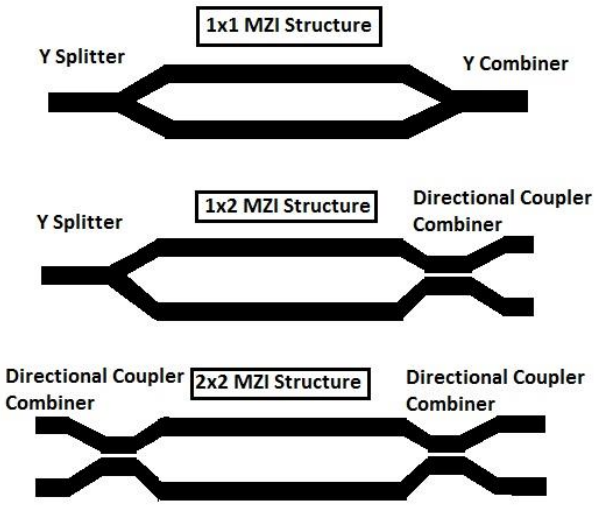

Figure 3-3: Three types of MZI structure first is 1 x 1 MZI structure, second is 1 x 2 MZI structure and last one is 2 x 2 MZI structure.

Our designs are based on the 2 x 2 MZI switch design or directional coupler splitter and directional coupler combiner. A full explanation of this design is given in following paragraphs.

3.5 MZI Switch Modulator

The MZI switch structure is shown below; it has two input waveguides (Inp1 and Inp2) and two output waveguides (Out1 and Out2) with two intermediate 3dB couplers used as a power splitter and combiner. It has three electrodes along with the interferometer arms (length L)[7],[26].

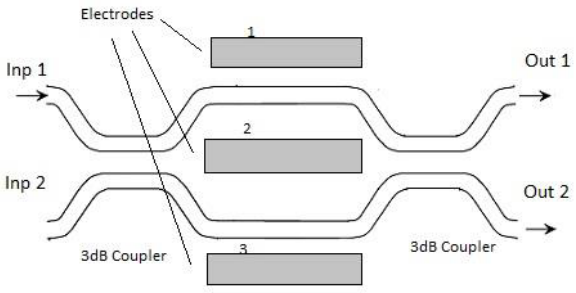

Figure 3-4: MZI Switch Modulator

Input optical signal gets split into two equal power optical signals by splitter. When an electrical field is applied on an interferometer branch, it produces a phase shift in

traveling optical signal because of Pockels effect. This phase change is converted to amplitude modulation by MZI structure of 2 x 2, if phase shift is zero, then both signal gets combine back. And if phase shift is 180 degrees then both signals cancel each other resulting in no signal output[27].

The phase change ($\Delta\varphi$) equation for the propagation through the interferometric arms can be given as[28].

$$\Delta\varphi = \frac{2\pi(\Delta n)}{\lambda} \tag{8}$$

Where L is the interferometer arm length and Δn is the change in refractive index due to the applied electrode voltage. When no voltage is applied to electrodes $\Delta\varphi$ is zero, and for a particular applied voltage if $\Delta\varphi$ equal to π, then this particular voltage is known as V_π or switching voltage or half wave voltage and is given by below equation[28],[29].

$$V_\pi = \frac{\lambda d}{n^3 r L} \tag{9}$$

Where d is the distance between electrodes, n is the refractive index of the material and r is the electro-optic coefficient. The normalized power at output ports is given as,

$$P_{out1} = sin^2\left(\frac{\Delta\varphi}{2}\right) \tag{10}$$

$$P_{out1} = cos^2\left(\frac{\Delta\varphi}{2}\right) \tag{11}$$

Here P_{out1} gives the output power at out 1 and P_{out2} gives the output power at Out 2. The input power is applied at Inp1 which is split into two equal parts by the 3dB coupler. If there is no applied electric field at the interferometer arms, then phase change will be zero, thus by above power equations no power reaches at Out 1 and all power is at Out 2 and if $\Delta\varphi$ is π for an applied voltage V_π, then maximum power is at Out1 and no power is obtained at Out 2.

To use this switch as a modulator, only one output port power is to be considered, and other is to be discarded. For that port, the insertion loss (I.L) and extinction ratio (Ex.R) to be calculated by the following equations[28].

$$I.L\ (dB) = 10\log_{10}\left(\frac{P_{out}}{P_{in}}\right) \quad (12)$$

$$Ex.R\ (dB) = 10\log_{10}\left(\frac{P_{on}}{P_{off}}\right) \quad (13)$$

Here P_{on} is the output power for input high, or '1' and P_{off} is the output power for input low, or '0'. In this project, this kind of MZI switch modulator is implemented for the visible light communication at visible wavelengths with reasonable small size.

Chapter 4 Design Tool: OptiBPM and MZI Switch Design Implementation

4.1 Introduction

This chapter is a brief introduction to the OptiBPM tool. Expanded form of name OptiBPM is Optical Beam Propagation Method. OptiBPM is the product of Optiwave Company based in Ottawa, Canada. It is a useful tool for designing the integrated photonics devices. By using OptiBPM this project is designed, and the designing process of MZI switch is explained.

4.2 OptiBPM

OptiBPM is the product of Ottawa, Canada Based Company 'Optiwave' which is a leading software organization in the integrated photonics sector. The OptiBPM is an integrated CAD environment tool used for the design of optical waveguides. Based on the Beam Propagation Method (BPM) to simulate the passageway of light through any waveguide means, OptiBPM permits designers to spot computer simulation by illuminating light[30].

OptiBPM is a potent and accessible software system that permits to make a design for a variety of integrated guided wave and fiber problems on your computer. Beam propagation process (BPM) is a step-by-step procedure that simulates the passageway of light through each waveguiding medium. A field can be checked at any time as it propagates along a fiber-driver integrated optical structure. BPM allows spotting computer-simulated light distribution field. You can view the radiation field and concurrently drive it[31].

In the OptiBPM layout, data can be entered very smoothly. It comprises tools of waveguide editing, special layout regions, primitive and tool of manipulation. The propagation of light can be simulated in 2D and 3D waveguide devices by this tool[32]. Simulation can be done using following methods.

In 2D are

1. X-directions(Vertical)- Transversal
2. Z- directions (horizontal)- Propagations

3D are

1. X-directions (verticals)- Transversal
2. Y- directions (Depth)
3. Z- directions (horizontal)- Propagations

The simulated device has step similar to refractive index distribution in transversals dimensions. To obtain a 2D device from a real 3D device, applying the effective rate method. The 3D reduction in 2D is the replacement of 2D cross-section of the 1D cross-section device. The genuine cross-sectional index is substituted by a 1D in effect index distribution. Though the actual index method is an estimated solution works on several devices. BPM in 3D input data modeling comprises of the distribution of the diffusion index of the start propagation field and a series of digital parameters. Refractive index and input field are defined while designing the layout of the device and other fields like starting field are defined in Global data pop up while simulating the same.

The OptiBPM handling environment includes as a key element of the Beam Propagation Method (BPM), as the best solutions that are well-suited with BPM algorithms. The BPM considers the monochromatic signals associated with the resolution of the Helmholtz equation. Propagation models built on the Helmholtz equation approach used.

4.2.1 2D BPM

The 2D BPM is based on the Crank-Nicolson algorithm of FDM. Here we can adjust following program parameters in the simulation:

- Polarization choice in TE and TM
- Starting field angle availability
- Boundary conditions are TBC (Transparent) and PLM (Perfectly Matched Layer)

- Options for starting field like rectangular field, Gaussian field, waveguide mode, and user field.
- RI options are user defined, modal and average.
- Propagation can be wide angle.

4.2.2 3D BPM

3D BPM works on

- Scaler algorithm
- Choices are between quasi-TE and quasi-TM
- ADI (Alternate Direction Implicit) scheme
- Fully vectors algorithms

4.2.3 Mode Solver

Following are the mode solvers for the 2D and 3D algorithms

1. ADI (Alternating directions implicit)
2. CFM (Correlation Functions Methods)
3. TMM (Transfer Matrix's Methods)

4.2.4 Graphics

The graphical features include:

- ✓ Structural view of the 3D results
- ✓ Colour altitude coding
- ✓ Solid modeling in 3D visuals
- ✓ Addition customizable colours

The finite difference Beam Propagation Modal (BPM) is a standout amongst the most intense strategies to explore straight and nonlinear light wave proliferation wonders in pivotally differing waveguides, for example, curvilinear directional couplers, stretching and joining waveguides, S-moulded twisted waveguides and decreased waveguides. BPM is additionally very essential for the examination of ultra-short light heartbeat spread in optical fibers.

Finite Diff. BPM solves the Maxwell equation by finite difference method instead of a derivative method.

4.3 OptiBPM Applications

OptiBPM have three application inbuilt in it

1. **OptiBPM layout designer**- Makes the layout and creates the **.bpd** file.
2. **OptiBPM Simulator**- It processes the **.bpd** file and makes a new **.bpa** file it shows the results while the simulation is in progress.
3. **OptiBPM Analyser-** It analyses the results from the simulator that means it analyses the **.bpa** file in depth details.

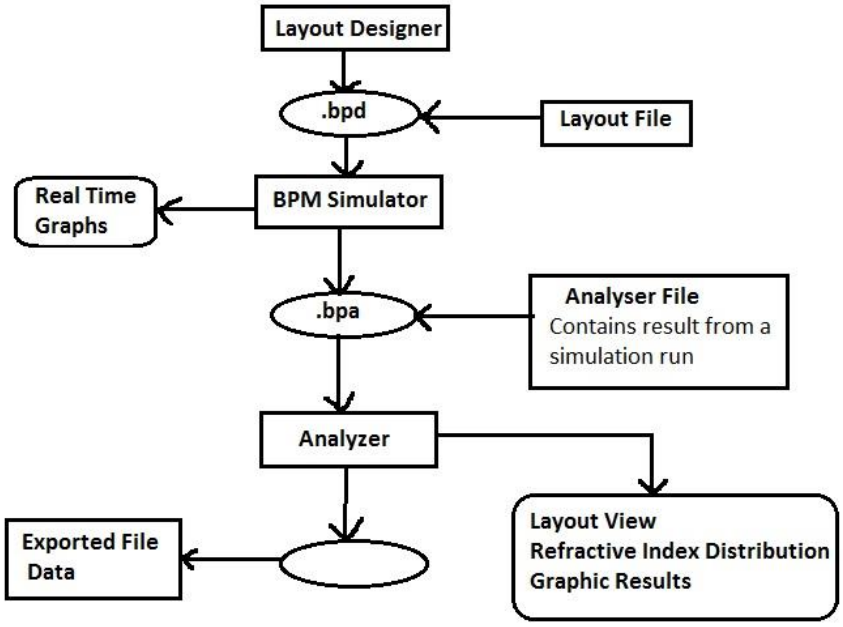

Figure 4-1: OptiBPM Applications flowchart

4.4 MZI Switch Designing Using OptiBPM

Here the process of making of Mach-Zehnder Interferometer based 2 x 2 switch is explained. The device is fabricated on Lithium Niobate substrate by Titanium diffusion in it. The switching of signal occurs because of electro-Optic effect within the structure by applying a switching voltage on the electrodes in the structure. Applied electrode voltage creates the variation in the refractive index. If it's properly designed then this variation in refractive index can induce different coupling in different individual ports. Here an example device with 33 mm length and 100μm width is designed[30].

Designing steps for the MZI switch are-

- ❖ CAD design for the device layout
- ❖ Defining the electrode region in the layout
- ❖ Input field defining and running the simulation

The procedure of making MZI design layout and running simulation is shown in following chart.

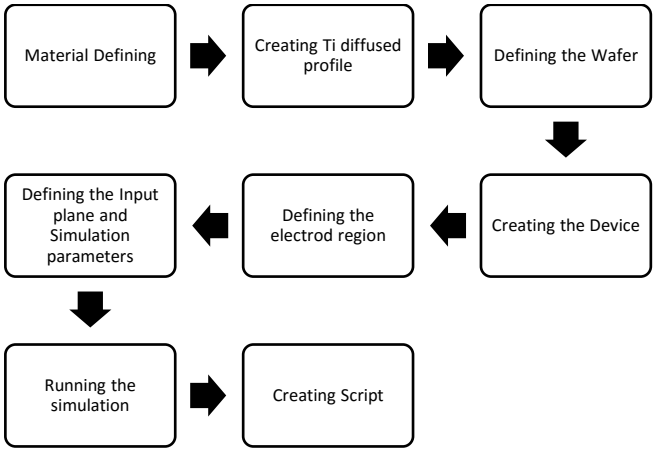

Figure 4-2: Flowchart of MZI switch designing

4.5 CAD design of the Device

The assumption made for the MZI switch designing are Lithium Niobate wafer with Z-cut and air cladding. This structure is sloping toward the Y-axis of the wafer. So here we defined the substrate materials and dielectric materials. Screen shot of OptiBPM designer 9.0 is given in the figure 4-3.

4.5.1 Defining Materials

For this, 'Profile Designer' to be opened then diffused and dielectric material should be defined with following parameters.

- Crystal name – LINBO3
- Cut – Z
- Propagation direction- Y

Dielectric material definitions are-

- Name- air
- RI (Re)- 1.0

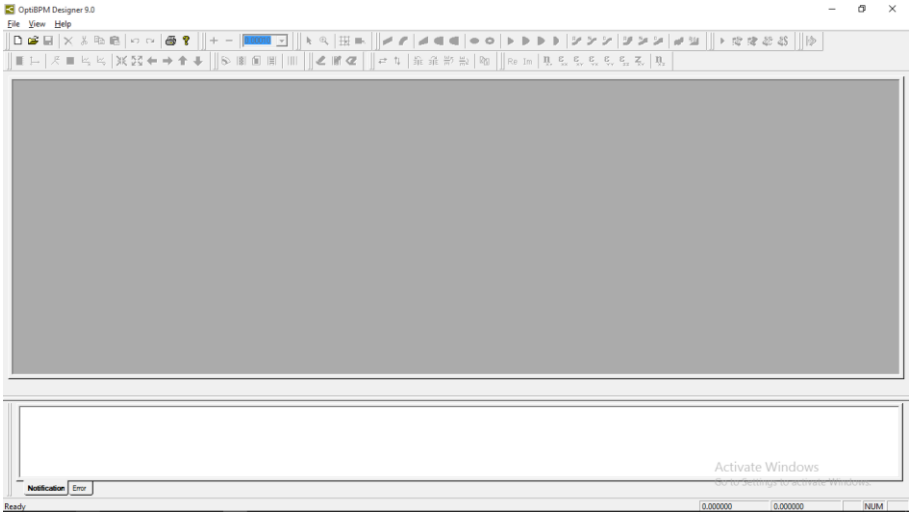

Figure 4-3: Screen shot of OptiBPM Designer

4.5.2 Creation of Ti diffused profile

To design the waveguides we use Ti diffused $LiNbO_3$ (Lithium Niobate)

- Profile Name- Ti_LINBO3
- Lateral diffusion length D_H is 3.5 µm
- Diffusion length depth D_V is 4.2 µm

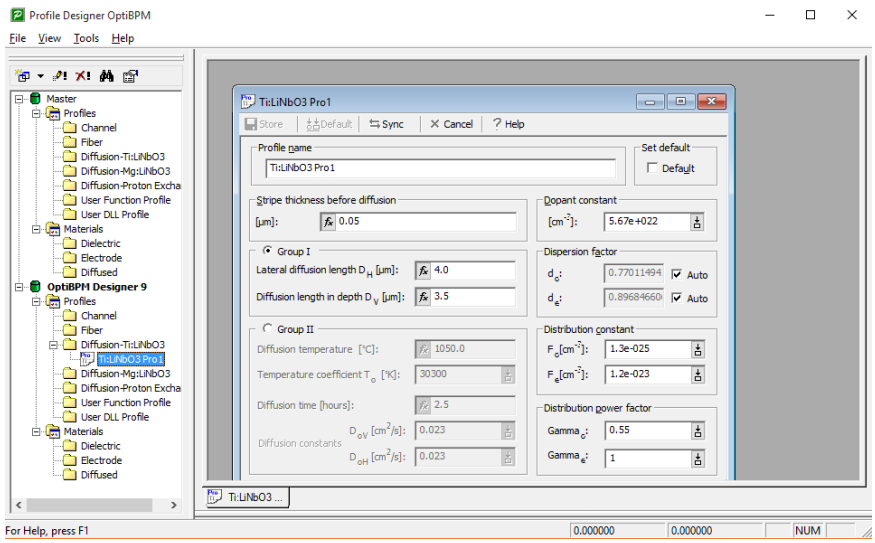

Figure 4-4: Profile Designer

4.5.3 Defining Wafer

The Wafer will be of 33 mm length and 100 µm width and it will be defined in the layout Designer in OptiBPM

Waveguide Properties

- Width 8 µm
- Profile as Ti_LINBO3

Wafer Dimensions will be

- Length 33000 µm
- Width 100 µm

In 2D wafer properties, refractive material will be LINBO3

In 3D wafer properties

- Cladding- air
- Cladding thickness- 2 µm
- Substrate material will be LINBO3 with 10 µm thickness

4.5.4 Creation of Device

For creating the device in the layout designer, we will draw following waveguides in the layout area

Table 4-1: Waveguide drawing positions

Waveguide	Start Position		End Position	
SBendSin1	Horizontal	0	Horizontal	5750
	Vertical	-20	Vertical	-7.25
Linear1	Horizontal	5750	Horizontal	9000
	Vertical	-7.25	Vertical	-7.25
SBendSin2	Horizontal	9000	Horizontal	11500
	Vertical	-7.25	Vertical	-16
Linear2	Horizontal	11500	Horizontal	21500
	Vertical	-16	Vertical	-16
SBendSin3	Horizontal	21500	Horizontal	24000
	Vertical	-16	Vertical	-7.25
Linear3	Horizontal	24000	Horizontal	27250
	Vertical	-7.25	Vertical	-7.25
SBendSin4	Horizontal	27250	Horizontal	33000
	Vertical	-7.25	Vertical	-20

By using above values, designed layout will look like figure 4-5. This structure will be flipped and mirrored in the above section and structure will be completed. The complete structure is shown in the figure 4-6.

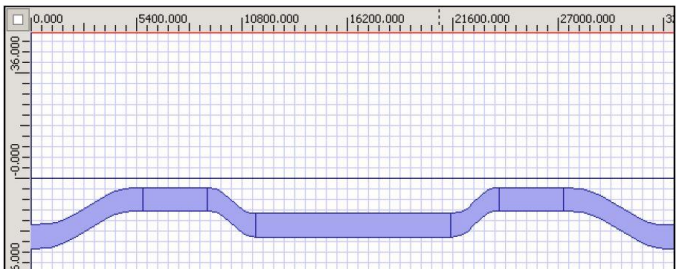

Figure 4-5: Only lower part of MZI layout

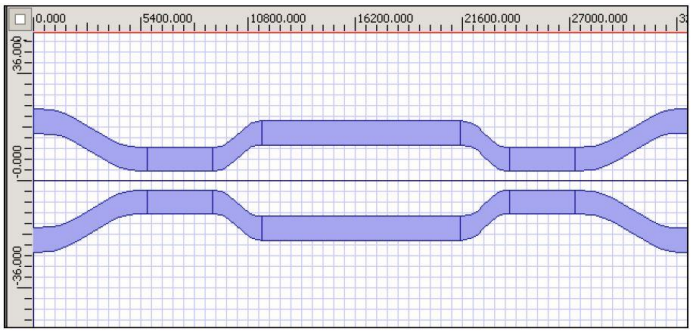

Figure 4-6: Both parts after mirror and copy

4.6 Defining the Electrode Region

To define the electrode region we have to open electrode region window in layout designer. Electrode region will start from 11500 µm and ends to 21500 µm in Z positioning. To draw the electrode region we will use a material named as 'buffer' with a refractive index of 1.47, it has to be defined in the profile designer. For use as electrode for structure following properties should be given to buffer-

- Thickness should be 0.3 µm and Electrode thickness should be 4 µm
- Horizontal and Vertical permittivity should be 4 µm

In addition to this, we have to add Electrode sets with following parameters

- Electrode 1, width 50 µm and Voltage 0 V.
- Electrode 2, width 26 µm and Voltage 0 V.

- Electrode 3, width 50 µm and Voltage 0 V.
- Gap between 1 and 2 is 6 µm and between 2 and 3 is 6 µm.
- Electrode 2 center position is 5.5 µm.

These three electrodes would get drawn over the layout in the layout designer; this is shown in following figure.

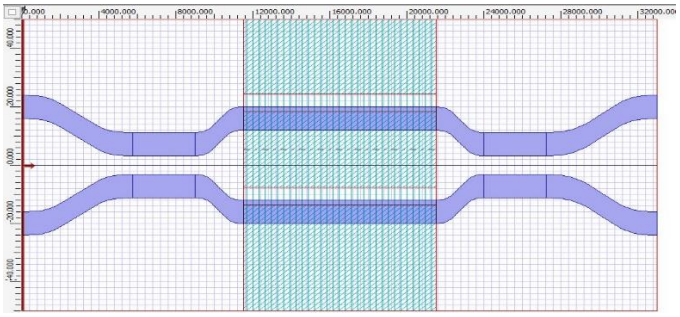

Figure 4-7: MZI switch layout with electrode region

4.7 Defining Input Plane and Simulation Parameters

To draw the input plane in the design, we will use draw input plane icon in the icon bar. After drawing input plane, we have to open the properties box of input plane and then select starting field to 'Mode' and Z position offset to 0.0 µm. Now in input fields 2D we have to add input at second waveguide.

To define the simulation parameters we have to open simulation parameter dialog box and set the data as follows.

- Reference Index should be Modal and wavelength 1.3 µm

2D simulation parameters should be as follow-

- Polarization should be TM
- Mesh numbers-500
- Paraxial BPM solver
- Finite difference engine
- Scheme parameter 0.5 and propagation step should 1.3 with TBC boundary conditions

4.8 Running the Simulation

To run the simulation for the designed device, we have to select simulation and calculate 2D isotropic simulation and then run. This will open OptiBPM Simulator and will show the running simulation and results of the simulation. We have run this design for electrode voltage (At electrode 2) at 0 V and at the switching voltage 6.75 V, both the results have been shown in the following figure.

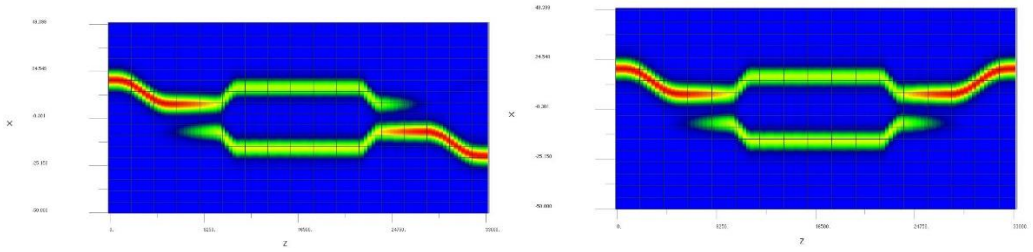

(a) (b)

Figure 4-8: Simulation result (a) at 0 switching voltage, and (b) at 6.75 switching voltage.

We can perform more optimization and investigate by using the scripting. We can scan the electrode 2 voltage for observation of output ports and to found waveguide mode behaviour. To use scripting we have to create a variable for the electrode voltage at electrode 2 or central electrode. This variable to be created in simulation and edit parameter window, let the name of the variable is V2. This variable should be made the voltage applied to the electrode 2 in edit electrode box. To run this type of simulation power in output waveguides Normalization to be chosen as Global and output type should be Power overlap with fundamental modes.

To create a script which runs simulation by varying V2 from 0.0 V to 7.2 V by the 0.8 V step. A simple scanning script can be written as-

```
Const NumIterations=10
ParamMgr.SetParam “V2”, 0.0
For x=1 To Numiterations
    ParamMgr.Simulate
    ParamMgr.SetParam “V2”, 0.8*x
    WGMgr.Sleep(50)
Next
```

Now we have to run the design with scanning script in simulation 2D isotropic simulation and have to select scanning using script option. This simulation will give results in OptiBPM Simulator and then will ask for opening OptiBPM Analyser by opening OptiBPM analyser we can examine all the iterations that we have run. By using Analyser application, we can find the Optical Power Propagation at any point in the device in any iteration of scripting. Following figure shows the output power variation at output ends at different iterations.

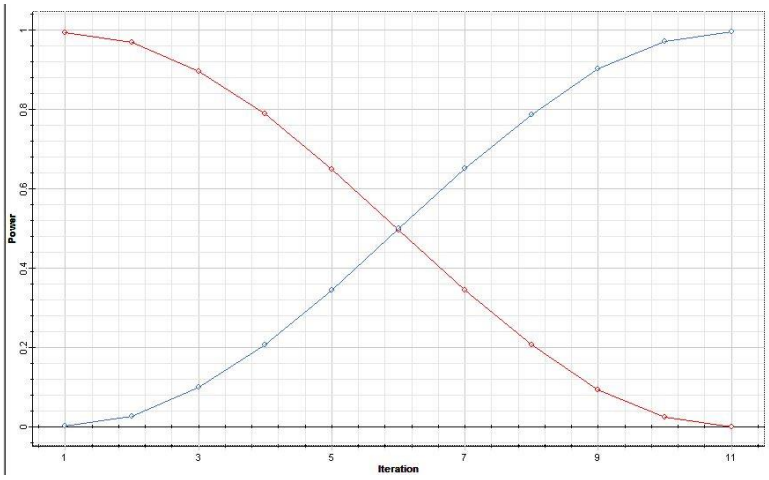

Figure 4-9: Power at output waveguides

By using above figure, we can find the output power value at the output ends and the value of switching voltage can be determined using it. By finding the power values, we can calculate important parameters Insertion Loss and Extinction Ratio.

Chapter 5 Compact MZI Switch Modulator for Visible Wavelengths

5.1 Introduction

The MZI switch modulator for visible wavelengths is discussed in this chapter. Designs which I have developed are given in details with the simulation results and required parameters. By using these results, Insertion Loss and Extinction Ratio of designs are calculated. These modulators are designed using OptiBPM software which is explained in chapter 4. We have discussed about 6 mm and 4 mm designs which very compact and shows the high value of extinction ratio along with the little value of insertion loss.

Following six modulators have been developed and proposed for the use in visible light communication (except first design which works at1300 nm):

- 33 mm long, operating at 1300 nm
- 33 mm long, operating at 680 nm
- 8 mm long, operating at 680 nm
- 6 mm long, operating at 610 nm
- 4.5 mm long, operating at 515 nm, and
- 4 mm long, operating at 515 nm

Detailed explanation of each design is given in the following subsection with important parameters like Insertion Loss and Extinction Ratio Calculation.

5.2 33 mm design operating at 1300 nm

This design is the commercial available MZI switch modulator which works at 1300 nm wavelength reported in [7]. Designing process for this design is same as explained in chapter 4 subsection 4.4. The wafer size for this design is 33000 µm length and 100 µm width; waveguide profile is Titanium diffused on Lithium Niobate. Properties of Lithium Niobate material are given in the following screen shot. Here the refractive indices are

Ordinary r_o =*2.22* and Extraordinary r_e=*2.14*, and Electro-Optic coefficients are r_{33}= 30.8 (10^{-12} m/V), r_{13}=8.6 (10^{-12} m/V), r_{15}=28 (10^{-12} m/V), r_{22}=3.5 (10^{-12} m/V). Permittivities are Eps=28, and Eps=43.

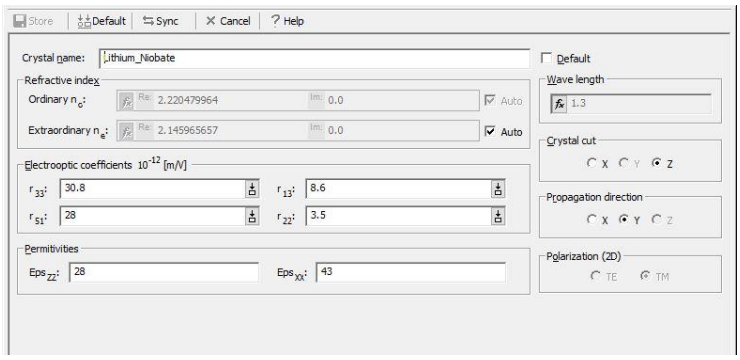

Figure 5-1: Optical properties of Lithium Niobate

Design parameter for the 33 mm switch modulator are-

- Crystal Cut Z, Propagation Direction is Y, Air is the dielectric material, Waveguide profile is Ti:$LiNbO_3$
- Wafer length is 33 mm and width is 100 µm, Waveguide width is 8 µm, Electrode length is 10 mm, Electrode material has Refractive index of 1.47, and Electrode thickness is 4 µm. Gap between electrodes is 6 µm and centre position is 5.5 µm
- Interferometer arm gap is 32 µm and coupler arm gap is 14.5 µm.

Layout design using above parameters is shown in the following figure.

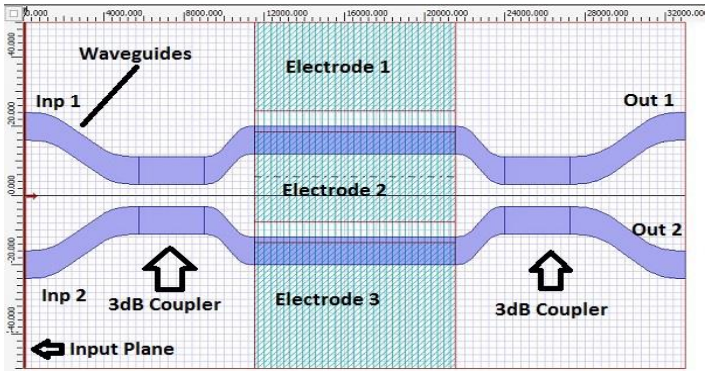

Figure 5-2: Layout of 33 mm design

The simulation environment for the above design can be given by following simulation parameters.

- Simulation has been run using 2D BPM, Modal type of starting field has been chosen at Z=0 value. Simulation wavelength is 1300 nm and Global refractive index is also Modal type with value 2.147.
- TM polarization has been used with 500 mesh points, Paraxial BPM solver is used with Finite Difference engine, Scheme parameter is 0.5 and propagation step is 1.3 with boundary conditions TBC (Transparent Boundary Conditions

After running this simulation, we get optical field propagation in the waveguides, for no voltage applied at interferometer branch, this will give following propagation direction.

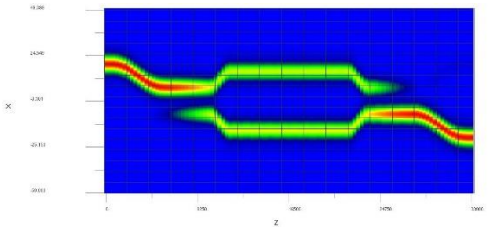

Figure 5-3: Optical field propagation at 0 electrode voltage

To find the switching voltage for this design, we have run simulation using a script which varies switching voltage from 0 V to 7.2 V with the step of 0.8 V. The script is given in the chapter 4 subsection 4.8. This simulation provides the switching voltage (V_π) at 6.75 V. For this value Optical field propagation is given below where we can found the switching of optical power from one port to another port.

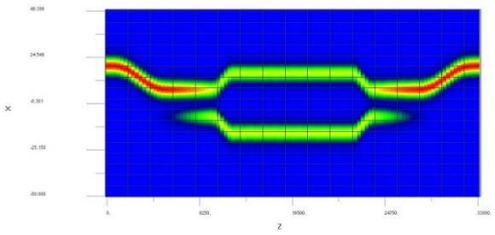

Figure 5-4: Optical Field after switching

In the first figure where no electrical field is applied to the interferometer branch, no phase variation happens in electrode region thus optical power transfer occurs using following equations of power output at output end.

$$P_{out1} = sin^2\left(\frac{\Delta\varphi}{2}\right)$$

$$P_{out1} = cos^2\left(\frac{\Delta\varphi}{2}\right)$$

So when no phase change means zero phase change, which will result in all power reach at Out 2, and no power at Out 1. When we apply electrical field at electrode 2, it will create refractive index change in the interferometer branches because of electro-optic effect. When applied electrical voltage at a particular value that induces the phase change of π, this phase variation will result in switching of power output at the output ends. This particular voltage is known as the half wave voltage or switching voltage (V_π).

The power variation in output waveguides is given below, by using this plot we can find the value of output power at Out 1 and Out 2.

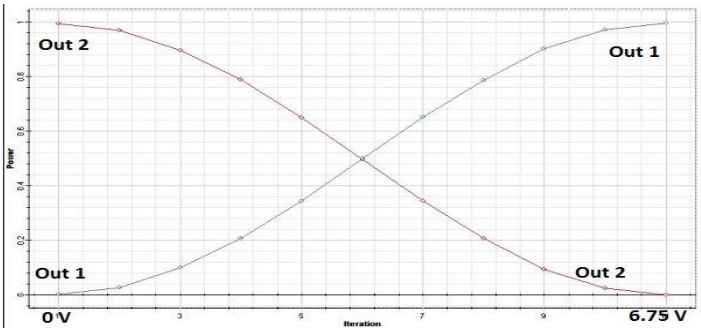

Figure 5-5: Power at output ends v/s electrode voltage

To find the value of output power at output port, we will open information window and then zoom in the above plot in the OptiBPM analyser. After that we have to put a marker at the point where we want to find the value of power, an example of that procedure is shown below.

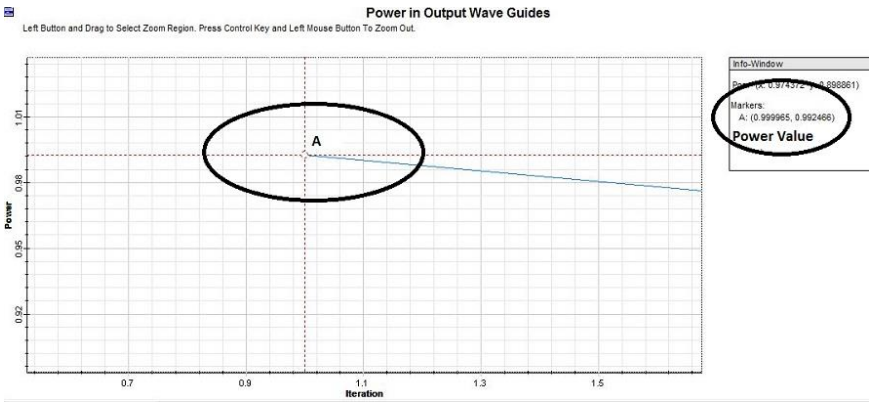

Figure 5-6: Power value at output ports

By using the above process, we have found the values of output powers for this design which are given below-

For 0 V switching voltage-

- P_{out1} is 0.00291 mW and P_{out2} is 0.99244 mW

For 6.75 V switching voltage-

- P_{out1} is 0.99556 mW and P_{out2} is 0.000064 mW

In the above results, the high value of P_{out} shows the P_{on} for corresponding input and low value of P_{out} gives the P_{off} value. By using these results, the insertion loss and extinction ratio have been calculated by using following equations

$$I.L\ (dB) = 10\log_{10}\left(\frac{P_{out}}{P_{in}}\right)$$

$$Ex.R\ (dB) = 10\log_{10}\left(\frac{P_{on}}{P_{off}}\right)$$

The value of P_{in} for all designs is 1 mW. Calculated value of insertion loss for Out 1 is 0.0193 dB and for Out 2 it is 0.0329 dB, Extinction ratio of the above design calculated to 25.34 dB for Out 1 and 41.90 dB for Out 2.

Thus by considering these results, we can say port 2 that is Out 2 have higher value of extinction ratio in comparison to port 1 i.e. Out 1. So this port should be used as the output of the MZI switch modulator. Switching voltage (V_π) for this design is 6.75 V and the length of ferrometer arm (L) is 10 mm, hence using these values we will have switching voltage- length product ($V_\pi L$) at 6.75 Vcm.

Cut view of output ends for zero switching voltage and 6.75 V switching voltage is shown below. These shows the position of output port end at the wafer width along with the value of propagating electrical field.

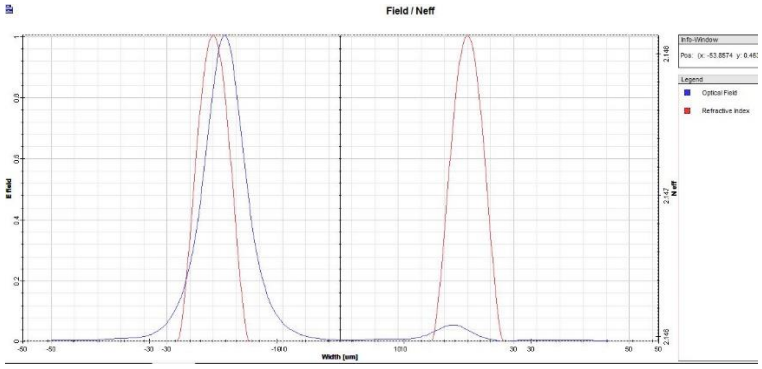

Figure 5-7: Field and Effective refractive index for Vπ=0 V

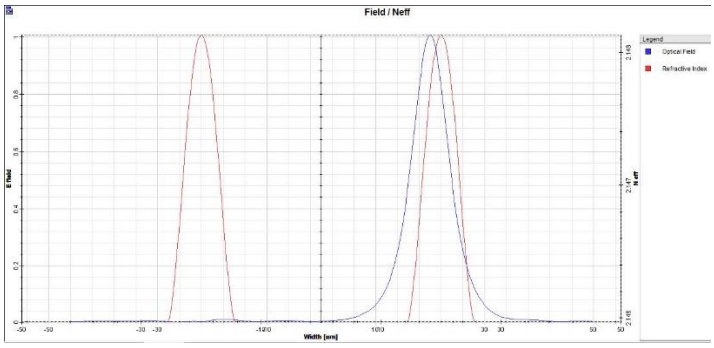

Figure 5-8: Field and Effective refractive index for Vπ=6.75 V

5.3 33 mm design operating at 680 nm

This design is proposed by me in the first assignment of my project. Here the length of the wafer is 33 mm and width is 100 µm, which is same as the previous design. I have worked to make it work at visible wavelengths. In order to do that I have optimized the distance between coupler arms and found the switching voltage for the design. The material used in this design is same Titanium diffused Lithium Niobate (Ti: $LiNbO_3$) and cladding material is air with refractive index value 1. Design parameters are same as the previous design except the gap between coupler arms is 10 µm and operating wavelength is 680 nm. Layout for this design is same as shown in Figure 5-2.

For simulation, parameters used are the same as the previous design except the wavelength 680 nm and switching voltage which is found to be 2 V. Simulation results for this design are explained in the subsequent sections with obtained plots and diagrams.

Optical field propagation over the switch modulator are shown in the following figures.

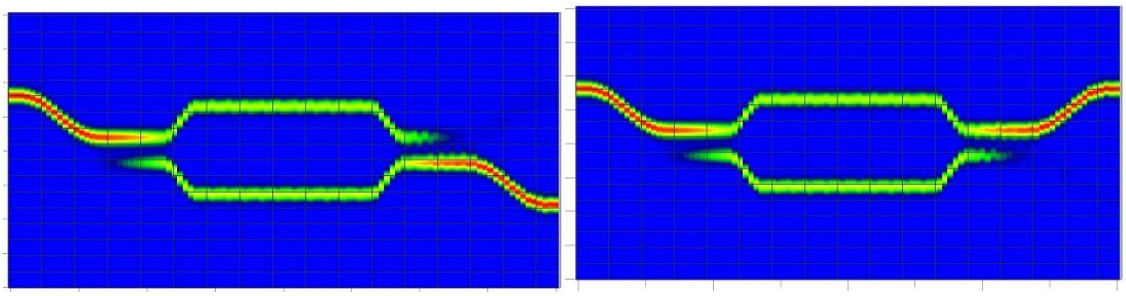

(a) (b)

Figure 5-9: Optical field propagation for (a) Vπ= 0 V and for (b) Vπ= 2 V

Power in output waveguides versus applied electrode voltage is shown in Figure 5-10. Here we can found the switching voltage V_π at 2 V, the value of power at output ends are found as For 0 V switching voltage-

- P_{out1} is 0.0349 mW and P_{out2} is 0.9565 mW

For 2 V switching voltage-

- P_{out1} is 0.8864 mW and P_{out2} is 0.0281 mW

Calculated value of insertion loss for Out 1 is 0.5234 dB and for Out 2 it is 0.1927 dB, Extinction ratio of the above design calculated to 14.04 dB for Out 1 and 15.31 dB for Out 2.

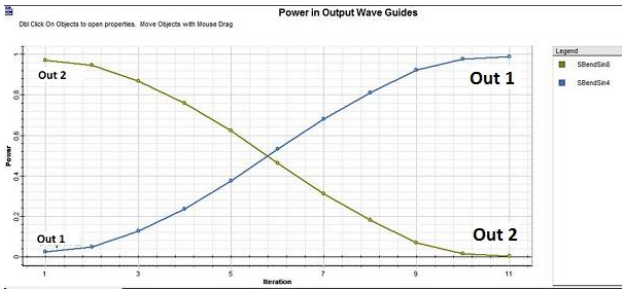

Figure 5-10: Power in output waveguides versus applied electrical field

Thus this design works on wavelength 680 nm with switching voltage 2 V which is quite lower than previous value 6.75 V. But the value of extinction ratio is low compared to previous design. The product $V_\pi L$ is 2 Vcm for this design which is good as compared to previous modulator design.

5.4 8 mm Design operating at 680 nm

This MZI switch modulator is approximately 4 times smaller than the previous designs, it operates at wavelength 680 nm and has the switching voltage value 6.4 V. The wafer dimensions of this design are 8 mm length and 80 µm width. The length is decreased significantly from previous design. Layout of this design is given in following figure.

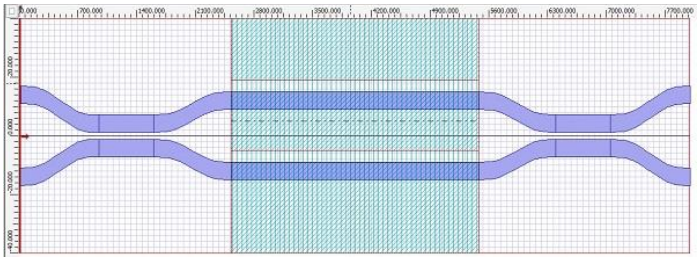

Figure 5-11: Layout of 8 mm design operating at 680 nm

Design parameter for the 8 mm switch modulator are-

- Crystal Cut Z, Propagation Direction is Y, Air is the dielectric material, Waveguide profile is Ti:$LiNbO_3$
- Wafer length is 8 mm and width is 80 µm, Waveguide width is 6 µm, Electrode length is 2.95 mm, Electrode material has Refractive index of 1.47, and Electrode thickness is 4 µm. Gap between electrodes is 4 µm and centre position is 5 µm
- Interferometer arm gap is 24 µm and coupler arm gap is 8.32 µm.

Simulation Parameters are as follow-

- Simulation has been run using 2D BPM, Modal type of starting field has been chosen at Z=0 value. The input field is applied at the input port 1 or Inp 1. Simulation wavelength is 680 nm and Global refractive index is also Modal type with value 2.147.
- TM polarization has been used with 500 mesh points, Paraxial BPM solver is used with Finite Difference engine, Scheme parameter is 0.5 and propagation step is 1.3 with boundary conditions TBC (Transparent Boundary Conditions.
- Simulation has been run using scripting to analyse the results in more details.

By running simulation, we get optical field as follow.

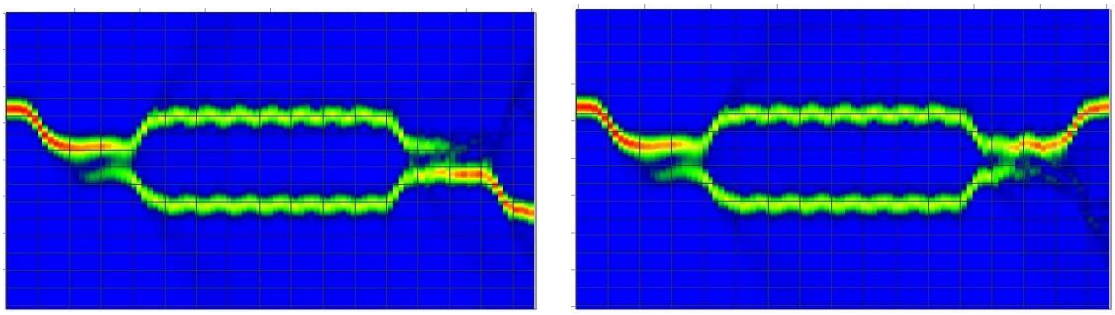

(a) (b)

Figure 5-12: Optical field propagation of 8 mm design with (a) Vπ= 0 V, and (b) Vπ= 6.4 V

OptiBPM analyser output of this design gives the Power in output waveguides versus applied electrode voltage curves. By observing these, we have found the value of power at output ends at different value of applied voltage. These values are-

- For 0 V switching voltage P_{out1} is 0.0070 mW and P_{out2} is 0.8672 mW
- For 6.4 V switching voltage P_{out1} is 0.8734 mW and P_{out2} is 0.0014 mW

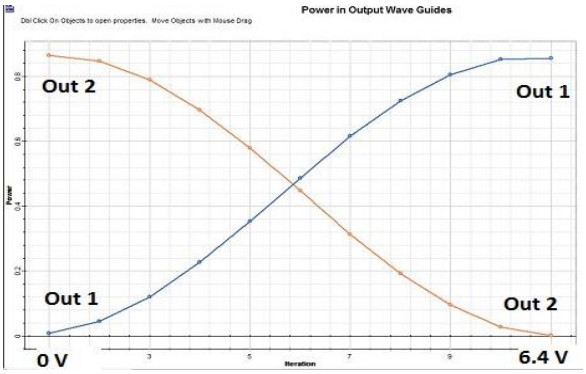

Figure 5-13: Power at output waveguide

Calculated value of insertion loss for Out 1 is 0.5875 dB and for Out 2 it is 0.6184 dB, Extinction ratio of the above design calculated to 20.91 dB for Out 1 and 27.67 dB for Out 2. Thus design has good extinction ratio for both ports while Out 2 shows the high extinction ratio in comparison to Out 1 that means a lower probability of errors in transmission. The insertion loss for both the designs is approximate same around 0.6 dB which lower than 1 dB. The value of $V_\pi L$ is 1.888 Vcm.

5.5 6 mm Design Operating at 610 nm

After designing the 8 mm design, I worked to reduce the size and to change its operating wavelength, in this process a design with 6 mm length have been found which works on the 610 nm wavelength. Thus the wafer size gets further reduced to 6 mm length and 80 µm width.

Design parameters are same as the above 8 mm design with some variations as follow.

- Wafer length is 6 mm and width is 80 µm, Waveguide width is 4.5 µm, Electrode length is 2.6 mm, Electrode material has Refractive index of 1.47, and Electrode thickness is 4 µm. Gap between electrodes is 4 µm and centre position is 4 µm
- Interferometer arm gap is 16 µm and coupler arm gap is 7 µm.

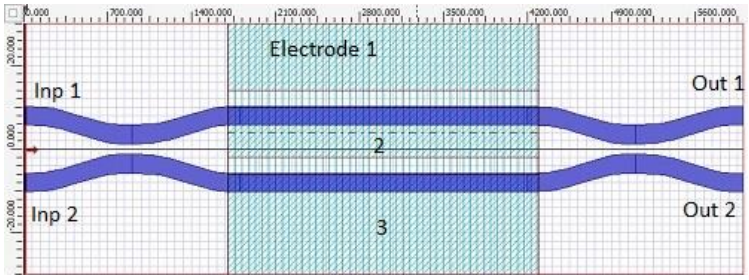

Figure 5-14: Layout of 6 mm design

Simulation parameters for this 6 mm MZI switch modulator design are same as the 8 mm design with just one change in simulation that is wavelength of 610 nm instead of 680 nm. The switching voltage is found to be 5.22 V for this design. In simulation results, the Optical field propagation is shown below.

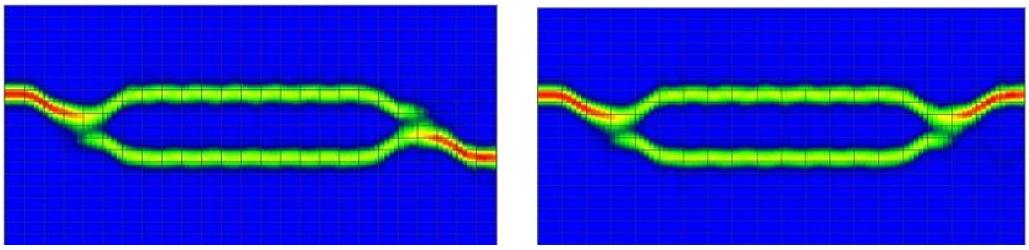

(a) (b)

Figure 5-15: Optical field propagation in 6 mm design (a) Vπ= 0 V, and (b) Vπ= 5.22 V

The power in output waveguides analysed by analyser gives the value of power at different output port. These values are-

- For 0 V switching voltage P_{out1} is 0.0003 mW and P_{out2} is 0.9841 mW
- For 5.22 V switching voltage P_{out1} is 0.9813 mW and P_{out2} is 0.0040 mW

In this modulator values of Insertion loss are calculated to 0.0819 dB for Out 1 and 0.0692 dB for Out 2, while the values of extinction ratio are calculated to 45.14 dB for Out 1 and 23.84 dB for Out 2. By observing the values of extinction ratio, we can conclude that Out 1 has the high extinction ratio in comparison to other port. Insertion loss for both the port is very low, value after two decimal points. The value $V_\pi L$ is 1.357 Vcm which is less than above designs.

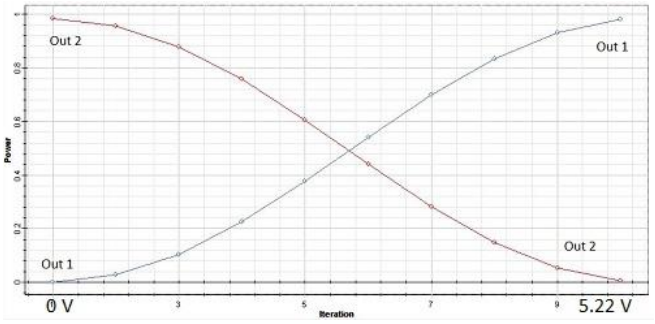

Figure 5-16: Power in output waveguide for 6 mm design

5.6 4.5 mm Design Operating at 515 nm

In order to further reduce the size and changing the value of operating wavelengths, a new design has been proposed with the length of 4.5 mm that operates at the 515 nm wavelength. For this modulator, the wafer size is 4.5 mm length and 60 µm width.

Design parameters are same as 6 mm design, but some variation are there in it, which are as follows-

- Wafer length is 4.5 mm and width is 60 µm, Waveguide width is 4 µm, Electrode length is 1.7 mm, Electrode material has Refractive index of 1.47, and Electrode thickness is 4 µm. Gap between electrodes is 4 µm and centre position is 3.7 µm
- Interferometer arm gap is 13.4 µm and coupler arm gap is 6.6 µm.

Layout for this design is given below.

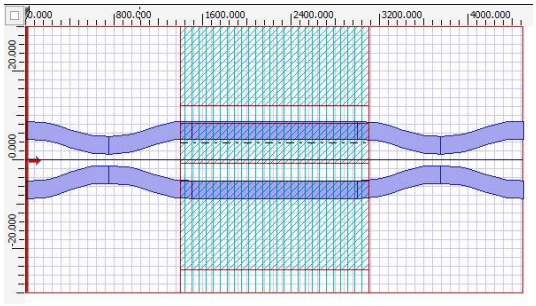

Figure 5-17: Layout of 4.5 mm design

Simulation parameters are also same as the previous 6 mm design but the simulation wavelength is 515 nm instead of 610 nm in above design. Simulated optical field propagation is shown in following figure. Switching voltage found to be 6 V which is higher than 6 mm design but lower than 8 mm design.

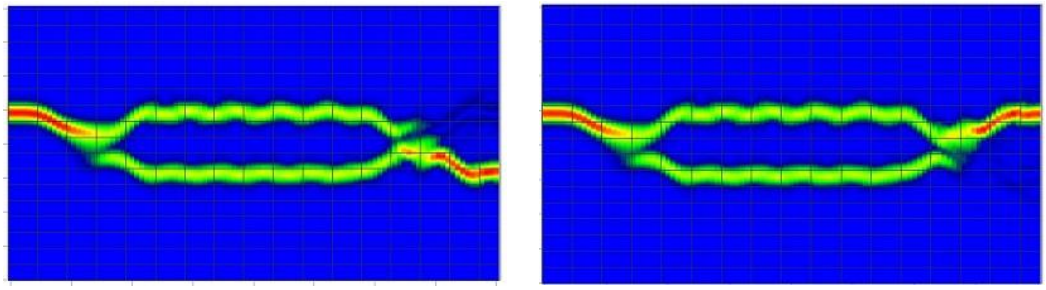

(a) (b)

Figure 5-18: Optical field propagation in 4.5 mm design (a) Vπ= 0 V, and (b) Vπ= 6 V

Power in output waveguides versus applied electrode voltage variation is shown in below plot.

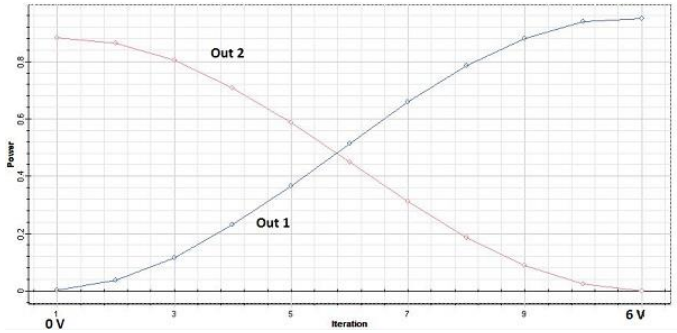

Figure 5-19: Power in output waveguides versus switching voltage plot

Power in output waveguides is found to be as-

- For 0 V switching voltage P_{out1} is 0.0020 mW and P_{out2} is 0.8831 mW
- For 5.22 V switching voltage P_{out1} is 0.9496 mW and P_{out2} is 0.00012 mW

In this modulator value of Insertion loss is calculated to 0.2242 dB for Out 1 and 0.5396 dB for Out 2, while the value of extinction ratio is calculated to 26.63 dB for Out 1 and 38.66 dB for Out 2. Extinction ratio at Out 2 is higher than the extinction ratio of Out 2 which that means Out 2 is a better choice to choose as modulator output port. Insertion loss at Out 2 is little higher than Out 1's insertion loss. The switching voltage-length product is found to be 1.02 Vcm, which is lowest in the above designed modulator devices.

5.7 4 mm Design Operating at 515 nm

Working on the size of MZI switch modulator for the visible wavelengths, I designed a modulator with 4 mm length, more than 8 times smaller than the reported 33 mm design. This design is the best design in this thesis work; it's the final design in this series of MZI switch modulator designs. The size of wafer is 4 mm length and 60 µm width.

Design parameter of this design is same as the 4.5 mm design but the length of interferometer and gap between waveguide branches is optimized to make switching possible. These optimised values are as follow-

- Wafer length is 4 mm and width is 60 µm, Waveguide width is 4 µm, Electrode length is 1.2 mm, Electrode material has Refractive index of 1.47, and Electrode thickness is 4 µm.
- Interferometer arm gap is 13.4 µm and coupler arm gap is 6.6 µm.

With these values layout of this design is given as follow-

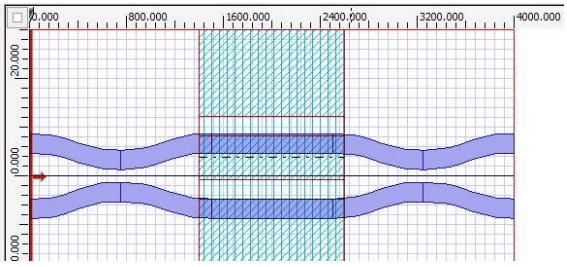

Figure 5-20: Layout of 4 mm MZI switch modulator design

Simulation parameter for this design are kept same as the simulation parameters of 4.5 mm design, and we found the value of switching voltage as 8 V. Simulation has been run using the scanning script in OptiBPM. Optical field propagation of this design is given below.

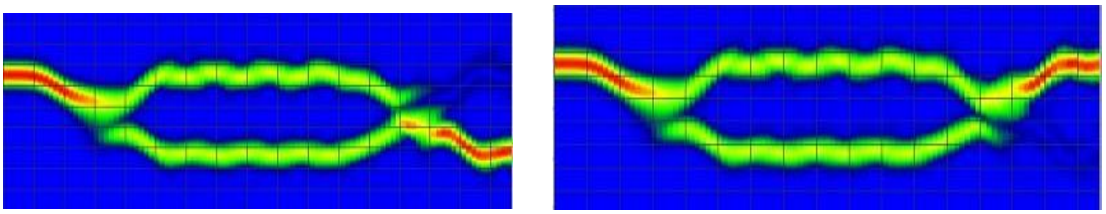

(a) (b)

Figure 5-21: Optical field propagation in 4 mm design (a) Vπ= 0 V, and (b) Vπ= 8 V

Simulation result of power in output waveguides versus applied electrode voltage at electrode 2 is given in following plot, by using this power at output port have been observed to calculate the insertion loss and extinction ratio.

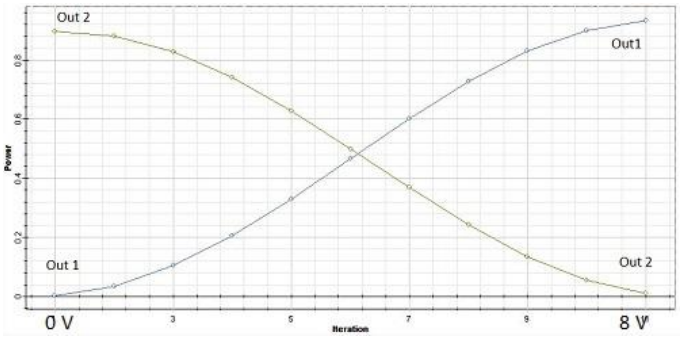

Figure 5-22: Output Power versus applied electric field variations

Values of power at output ends found to be-

- For 0 V switching voltage P_{out1} is 0.0027 mW and P_{out2} is 0.8969 mW
- For 5.22 V switching voltage P_{out1} is 0.9332 mW and P_{out2} is 0.0092 mW

These values of power at output ends gives the values of insertion loss and extinction ratio of this device. Calculated value of insertion loss for Out 1 is 0.3002 dB and for Out 2 it is 0.4722 dB, Extinction ratio of the above design calculated to 25.35 dB for Out 1 and 19.86 dB for Out 2. By observing these values, we can say that Out 1 is a better choice as output port choice for the MZI switch modulator because it has the lower

value of insertion loss and higher value of extinction ratio in comparison to other port Out 2. Switching voltage of this device is 8 V which is highest amongst the all designed modulators, but the value of $V_\pi L$ is 0.96 Vcm, which is lowest amongst all the designs.

This design is smallest among all designs and with the lowest value of parameter $V_\pi L$ that means finest design in term of power uses.

5.8 Comparison of Design Parameters

Table 5-1: Detailed comparison of the design parameters of modulator designs

Design Parameter	**33 mm at 1300 nm**	**33 mm at 680 nm**	**8 mm at 680 nm**	**6 mm at 610 nm**	**4.5 mm at 515 nm**	**4 mm at 515 nm**
Crystal Cut	Z	Z	Z	Z	Z	Z
Propagation Direction	Y	Y	Y	Y	Y	Y
Dielectric Material	Air	Air	Air	Air	Air	Air
Profile	Ti: $LiNbO_3$	Ti: $LiNbO_3$	Ti: $LiNbO_3$	Ti: $LiNbO_3$	Ti: $LiNbO_3$	Ti: $LiNbO_3$
Wafer length	33000 µm	33000 µm	8000 µm	6000 µm	4500 µm	4000 µm
Wafer Width	100 µm	100 µm	80 µm	80 µm	60 µm	60 µm
Waveguide Width	8 µm	8 µm	6 µm	4.5 µm	4 µm	4 µm
Electrode length	10000 µm	10000 µm	2950 µm	2600 µm	1700 µm	1200 µm
Electrode material Refractive index	1.47	1.47	1.47	1.47	1.47	1.47
Electro thickness	4 µm	4 µm	4 µm	4 µm	4 µm	4 µm
Inter electrode gap	6 µm	6 µm	4 µm	4 µm	4 µm	4 µm
Electrode centre position	5.5 µm	5.5 µm	5 µm	4 µm	3.7 µm	3.7 µm
Interferometer arm gap	32 µm	32 µm	24 µm	16 µm	13.4 µm	13.4 µm
Coupler arm gap	14.5 µm	14.5 µm	8.32 µm	7 µm	6.6 µm	6.6 µm

In above table, we can see the comparison of design parameters of all 6 modulator designs. The variation is found in the layout parameters with material and related properties are same.

5.9 Comparison of Simulation Parameters

Table 5-2: Comparison of Simulation parameters for the modulator designs

Simulation Parameter	**33 mm at 1300 nm**	**33 mm at 680 nm**	**8 mm at 680 nm**	**6 mm at 610 nm**	**4.5 mm at 515 nm**	**4 mm at 515 nm**
Simulation Type	2D Isotropic	2D Isotropic	2D Isotropic	2D Isotropic	2D Isotropic	2D Isotropic
Starting Field	Modal	Modal	Modal	Modal	Modal	Modal
Wavelength	1300 nm	680 nm	680 nm	610 nm	515 nm	515 nm
Global Refractive Index	2.147	2.197	2.196	2.211	2.245	2.245
Simulation Technique	Using script	Using script	Using script	Using script	Using script	Using script
Polarization	TM	TM	TM	TM	TM	TM
BPM Solver	Paraxial	Paraxial	Paraxial	Paraxial	Paraxial	Paraxial
Engine	Finite Difference	Finite Difference	Finite Difference	Finite Difference	Finite Difference	Finite Difference
Propagation Step	1.3	1.3	1.3	1.3	1.3	1.3
Boundary Condition	Transparent Boundary Condition	Transparent Boundary Condition	Transparent Boundary Condition	Transparent Boundary Condition	Transparent Boundary Condition	Transparent Boundary Condition
Switching Voltage	6.75 V	2 V	6.4 V	5.22 V	6 V	8 V

5.10 Comparison of Insertion Loss and Extinction Ratio

The comparison of Insertion Loss (IL) and Extinction Ration (ER) are given in tabular form, in the following table all values are in dB.

Table 5-3: Comparison of Insertion loss and extinction ratio of designed modulators.

Port	**33 mm at 1300 nm**		**33 mm at 680 nm**		**8 mm at 680 nm**		**6 mm at 610 nm**		**4.5 mm at 515 nm**		**4 mm at 515 nm**	
	IL (dB)	***ER (dB)***	***IL (dB)***	***ER (dB)***	***IL (dB)***	***ER (dB)***	***IL (dB)***	***ER (dB)***	***IL (dB)***	***ER (dB)***	***IL (dB)***	***ER (dB)***
Out1	0.0193	25.34	0.5234	14.04	0.5875	20.19	0.0819	**45.14**	0.2242	26.63	0.3002	**25.35**
Out2	0.0329	**41.90**	0.1927	**15.31**	0.6184	**27.67**	0.0692	23.84	0.5396	**38.66**	0.4722	19.86

By the above comparison of insertion loss and extinction ratio, we can decide the port for the use in modulator as output port. The port which has higher value of extinction ratio and lower value of insertion loss will be used as the output port in MZI switch modulator. We will prefer the port with high extinction ratio over the lower values of insertion loss comparison. For example in first design port Out 2 has high extinction ratio as compared to Out 1 but insertion loss is greater than Out 1, then we will choose Out 2 as an output port for the MZI switch modulator design.

5.11 Comparison of Switching Voltage and $V_\pi L$

Table 5-4: Comparison of Switching Voltage and VπL

Parameter	**33 mm at 1300 nm**	**33 mm at 680 nm**	**8 mm at 680 nm**	**6 mm at 610 nm**	**4.5 mm at 515 nm**	**4 mm at 515 nm**
V_π	6.75 V	2 V	6.4 V	5.22 V	6 V	8 V
$V_\pi L$	6.75 Vcm	2 Vcm	1.888 Vcm	1.357 Vcm	1.02 Vcm	0.96 Vcm

By observing above values of switching voltage and $V_\pi L$, we can say that in our proposed designs value of switching voltage is varying with operating wavelength and with length of design but the value of $V_\pi L$ is continuously decreasing with size reduction. Lower the value of this product means lower power consumption by the device hence more energy efficient.

Chapter 6 **Conclusion and Future Aspects**

In this work, some designs of MZI switch modulator are proposed to work at visible wavelengths. These designs can be used in visible light communication for the modulation purpose. We proposed 5 designs of modulators and optimized to work at visible wavelengths, in addition to this insertion loss and extinction ratio have been calculated. Magnitude of $V_{\pi}L$ product has been found for each modulator design.

Designs are compact and have low value of switching voltage-length product. Value of insertion loss is low for each design; it's less than 0.7 dB for every design. Extinction ratio is good for each design and its value is higher than 14 dB for each port, for one port it is as high as 45 dB in 6 mm design. We have achieved following properties for each design.

- In second 33 mm design which is able to operate at 680 nm wavelength, we have switching voltage 2 V and $V_{\pi}L$ is 2 Vcm, thus this device is very energy efficient in comparison to first reported 33 mm design which operates at 1300 nm and has the value of $V_{\pi}L$ at 6.75 V. But extinction ratio for this design is lowest in all the designs.
- In third 8 mm design, operating wavelength is 680 nm same as previous 33 mm design. This device has extinction ratio more than 20 dB for each port but the weak point with this device is that high value of insertion loss in comparison to all other modulator design.
- Fourth design which is of 6 mm length works on 610 nm lower than the previous value of 680 nm. Insertion loss is low in comparison to other designs which operates on visible wavelengths in our designs. The value of extinction ratio is up to 45 dB higher than the reported design of 33 mm at 1300 nm.
- Fifth design is more compact as 4.5 mm long and has the operating wavelength at 515 nm lowest among all the designs. The value of extinction ratio high up to 38.66 dB but value of insertion loss is high for this port.
- Last design is of length 4 mm and operating at the 515 nm wavelength; this design is compact in all modulator designs. It is more power efficient in comparison to

all devices because value of $V_\pi L$ is lowest amongst all the devices, the value of $V_\pi L$ is 0.96 Vcm which is very low to the value of $V_\pi L$ for reported 33 mm device.

In these designs, fourth design of 6 mm length operating at 610 nm and sixth design of 4 mm length operating at 515 nm are considered and proposed to use in VLC for modulation purpose. Reason for this is that 6 mm design has highest value of extinction ratio which is up to 45 dB and for the 4 mm design reason is its compact size and lowest value of $V_\pi L$.

Thus we have proposed two compact designs of MZI switch modulator to be used in visible light communication at visible wavelengths. These devices have high extinction ratio up to 45.14 dB in the 6 mm design with very low insertion loss. The switching voltage-length product is also very little in comparison to previous modulator designs. The low value of switching voltage-length product means compact and energy efficient device. These proposed modulator designs are a new idea for doing modulation in optical domain for VLC.

Future Aspect

In future, more improvement can be made in the MZI switch modulator designs. As these modulator designs are a new idea for modulation in optical domain in visible light communication system. Future work can be done on following parameters of these modulator designs-

- Size: size can be further reduced for this type of modulator design, compact size devices will result in more small VLC transmitters with lower power consumption.
- Switching Voltage: By reducing the switching voltage more power efficient designs can be made, reduction in switching voltage will result in a decrement of switching voltage length product parameter of MZI structure which is desirable.
- Insertion Loss: lower value of insertion loss for any device is desirable, by working on these design's one can reduce the value of insertion loss more than three digits after decimal point.

- Extinction Ratio: for any device extinction ratio must be high as possible, a higher value of extinction ratio results in lower chances of bit error in a communication system.
- Coupling: coupling in directional couplers should be equal in both the arms. This will result in an equal value of insertion loss and extinction ratio for both the output ports, at present these are not equal.

By working on the recommendation, more compact and power efficient modulator devices can be made. If these aspect can be met than industry level fabrication of this kind of modulator devices is possible to be used in visible light communication.

References

[1] D. C. O'Brien, L. Zeng, H. Le-Minh, G. Faulkner, J. W. Walewski, and S. Randel, "Visible Light Communications: Challenges and possibilities," *IEEE Int. Symp. Pers. Indoor Mob. Radio Commun. PIMRC*, pp. 1–5, 2008.

[2] L. U. Khan, "Visible light communication: Applications, architecture, standardization and research challenges," *Digit. Commun. Networks*, vol. 3, no. 2, pp. 78–88, 2016.

[3] Y. Ueda *et al.*, "Low Driving Voltage Operation of MZI-Type EA Modulator Integrated with DFB Laser Using Optical Absorption and Interferometric Extinction," *IEEE J. Sel. Top. Quantum Electron.*, vol. 21, no. 6, 2015.

[4] S. Haruyama, "Visible light communication using sustainable LED lights," *ITU Kaleidosc. Build. Sustain. Communities (K-2013), 2013 Proc.*, pp. 1–6, 2013.

[5] E. A. Shinwasusin, C. Charoenlarpnopparut, P. Suksompong, and A. Taparugssanagorn, "Modulation performance for visible light communications," *2015 6th Int. Conf. Inf. Commun. Technol. Embed. Syst. IC-ICTES 2015*, no. c, pp. 0–3, 2015.

[6] R. C. Alferness, "Titanium-Diffused Lithium Niobate Waveguide Devices," *Sixth IEEE Int. Symp. Appl. Ferroelectr.*, pp. 1–3, 1986.

[7] A. Kumar, S. Kumar, and S. K. Raghuwanshi, "Implementation of All-Optical Logic Gate using SOA-MZI Structures," *Trends in Opto Electro & Optical Communication, STM Journals*, pp. 13–21, 2013.

[8] N. A. Mohammed, H. S. A. Elnasr, and M. H. Aly, "Performance Evaluation and Enhancement of 2×2 Ti : $LiNbO_3$ Mach Zehnder Interferometer Switch at 1 . 3 μm and 1 . 55 μm," *Open Electr. Electron. Eng. J.*, vol. 6, pp. 36–49, 2012.

[9] J. Noda, M. Fukuma, S. Saito, and I. Introduction, "Effect of Mg diffusion on Ti-diffused $LiNbO_3$ a waveguides," *Journal of Applied Physics*, vol. 3150, no. February, pp. 3150–3154, 1978.

[10] T. H. Stievater *et al.*, "Enhanced electro-optic phase shifts in suspended waveguides," *Opt. Express*, vol. 18, no. 2, pp. 885–892, 2010.

[11] C. T. Zheng, C. S. Ma, X. Yan, X. Y. Wang, and D. M. Zhang, "Simulation and optimization of a polymer directional coupler electro-optic switch with push-pull electrodes," *Opt. Commun.*, vol. 281, no. 14, pp. 3695–3702, 2008.

[12] C. Zheng, C. Ma, X. Yan, X. Wang, and D. Zhang, "Analysis of response characteristics for polymer directional coupler electro-optic switches," *Opt. Commun.*, vol. 281, no. 24, pp. 5998–6005, 2008.

[13] Y. N. Zhao, G. Q. Zhang, Z. Z. Guo, S. Cheng, S. W. Li, and Z. G. Ma, "Application of pockels electro-optic effect in voltage transducer," *2012 Symp. Photonics Optoelectron. SOPO 2012*, 2012.

[14] K. Sala and M. C. Richardson, "Optical Kerr effect induced by ultrashort laser pulses," *Phys. Rev. A*, vol. 12, no. 3, pp. 1036–1047, 1975.

[15] M. R. Garcia, J. H. Galeti, R. T. Higuti, and C. Kitano, "A simple and efficient off-optical axis electro-optic voltage sensor," *2014 11th IEEE/IAS Int. Conf. Ind. Appl. IEEE INDUSCON 2014 - Electron. Proc.*, 2014.

[16] M. Passard, C. Barthod, M. Fortin, C. Galez, and J. Bouillot, "Design and optimization of a low frequency electric field sensor\nusing Pockels effect," *Proc. 17th IEEE Instrum. Meas. Technol. Conf. [Cat. No. 00CH37066]*, vol. 2, 2000.

[17] R. Weis and T. Gaylord, "Lithium Niobate: Summary of Physical Properties and Crystal Structure R.," *Appl. Phys. A Mater. Sci. Process.*, vol. 37, no. 4, pp. 191–203, 1985.

[18] E. L. Wooten *et al.*, "A review of Lithium Niobate modulators for fiber-optic\ncommunications systems," *IEEE J. Sel. Top. Quantum Electron.*, vol. 6, no. 1, pp. 69–82, 2000.

[19] L. Arizmendi, "Photonic applications of Lithium Niobate crystals," *Phys. Status Solidi*, vol. 201, no. 2, pp. 253–283, 2004.

[20] M. A. Metawe, A. Nabih, Z. Rashed, and A. M. Bendary, "Recent Progress of

$LiNbO_3$ Based Electrooptic Modulators with Non Return to Zero (NRZ) Coding in High Speed Photonic Networks," *International Journal of Information and Communication Technology Research (IJICT)*, vol. 1, no. 2, pp. 55–63, 2011.

[21] K. Noguchi, O. Mitomi, and H. Miyazawa, "Millimeter-wave Ti:$LiNbO_3$ optical modulators," *J. Light. Technol.*, vol. 16, no. 4, pp. 615–619, 1998.

[22] A. Rao *et al.*, "Heterogeneous microring and Mach-Zehnder modulators based on Lithium Niobate and chalcogenide glasses on silicon," *Opt. Express*, vol. 23, no. 17, p. 22746, 2015.

[23] R. C. Alferness, R. V Schmidt, and E. H. Turner, "Characteristics of Ti-diffused Lithium Niobate optical directional couplers.," *Appl. Opt.*, vol. 18, no. 23, pp. 4012–4016, 1979.

[24] K. X. Chen, X. P. Li, Y. L. Zheng, and K. S. Chiang, "Lithium-niobate Mach-Zehnder interferometer with enhanced index contrast by SiO2film," *IEEE Photonics Technol. Lett.*, vol. 27, no. 11, pp. 1224–1227, 2015.

[25] C. B. Bambhroliya, R. J. Thumar, and P. Sarman, "1 × 2 Digital Optoelectronic Switch using MZI structure and studying the Effect of Bi-Polar Voltage on Electrode," *International Journal for Scientific Research & Development (IJSRD)*, vol. 1, no. 8, pp. 600–603, 2013.

[26] G. Singh, V. Janyani, and R. P. Yadav, "Modeling of a high performance Mach-Zehnder interferometer all optical switch," *Optica Applicata*, vol. 42, no. 3, 2012.

[27] M. Lee, "Broadband Modulation of Light by Using an Electro-Optic Polymer," *Science (80-.).*, vol. 298, no. 5597, pp. 1401–1403, 2002.

[28] R. Khatun, K. T. Ahmmed, A. Z. Chowdhury, and R. Hossen, "Optimization of 2 x 2 MZI electro-optic switch and its application as logic gate," *2015 18th Int. Conf. Comput. Inf. Technol. ICCIT 2015*, no. December, pp. 294–299, 2016.

[29] S. Dubovitsky, W. H. Steier, S. Yegnanarayanan, and B. Jalali, "Analysis and improvement of Mach-Zehnder modulator linearity performance for chirped and tunable optical carriers," *J. Light. Technol.*, vol. 20, no. 5, pp. 886–891, 2002.

[30] Optiwave, "OptiBPM: Technical Background and Tutorials," *Waveguide Optics Modeling Software Systems,* version 12.2, 2014.

[31] Optiwave, "OptiBPM: Getting Started," *Waveguide Optics Modeling Software Systems,* version 12.2, 2014.

[32] Optiwave, "OptiBPM: User Reference," *Waveguide Optics Modeling Software Systems,* version 12.2, 2014.